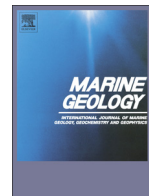




Contents lists available at ScienceDirect



Marine Geology

journal homepage: www.elsevier.com/locate/margo

Which earthquakes trigger damaging submarine mass movements: Insights from a global record of submarine cable breaks?

Ed L. Pope ^{a,*}, Peter J. Talling ^a, Lionel Carter ^b^a National Oceanography Centre, Southampton, European Way, Southampton SO14 3ZH, UK^b Antarctic Research Centre, Victoria University of Wellington, Wellington, New Zealand

ARTICLE INFO

Article history:

Received 23 July 2015

Received in revised form 14 January 2016

Accepted 18 January 2016

Available online xxxx

Keywords:

Submarine mass movements

Earthquakes

Cable breaks

Palaeoseismology

Peak ground acceleration

Hazards

ABSTRACT

Submarine landslides, debris flows and turbidity currents are significant geohazards for seafloor infrastructure in many locations around the world. Their deposits potentially provide a valuable record of major earthquakes, which extends further back in time than most terrestrial earthquake records. It is therefore important to determine their frequency and triggering mechanisms, and what types of earthquake trigger submarine slides and flows in different settings. Submarine cable breaks provided the first evidence of submarine mass movements, as shown by the 1929 Grand Banks earthquake. Even now the global network of subsea telecommunication cables provides our only means to monitor flows globally. Here, we present the first global analysis of the occurrence of submarine mass movements caused by earthquakes using cable break data. Using a global database of subsea fibre-optic cable breaks we identify earthquakes that triggered (and did not trigger) submarine mass movements from 1989 to 2015. We note that cable breaks are not a perfect record of submarine mass movements, and may only record more powerful ($>\sim 2 \text{ m s}^{-1}$) flows. However, our results show, in contrast to previous assertions, that there is no specific earthquake magnitude that systematically trigger mass flows capable of breaking a cable. Some earthquakes with magnitudes $> 7.0 \text{ M}_w$ triggered cable breaking flows, but many $> 7.0 \text{ M}_w$ earthquakes have failed to break nearby cables. We also show that some very small (3.0–4.0) magnitude earthquakes are capable of triggering cable breaking flows. The susceptibility of slopes to fail as a consequence of large and small earthquakes is dependent on the average seismicity of the region and the volume of sediment supplied annually in addition to other pre-conditioning factors such as slope architecture and mechanical sediment properties.

© 2016 Published by Elsevier B.V.

1. Introduction

Since the laying of the first submarine cables in 1842, this technology has acted as a detector of natural hazards in the ocean (Carter et al., 2012). Indeed, even now there have been relatively few studies where submarine mass movements have been directly monitored, and those that have are limited to only a few locations globally (Khripounoff et al., 2003; Andrieux et al., 2013; Cooper et al., 2013; Xu et al., 2014). The use of submarine cable breaks therefore still plays a crucial role in understanding submarine mass movements in different areas around the world (Heezen and Ewing, 1955; Heezen et al., 1964; El-Robrini et al., 1985; Piper et al., 1999; Hsu et al., 2008; Carter et al., 2012; Talling et al., 2014).

Turbidity currents, and other types of submarine sediment density flow (Talling et al., 2012) can travel at speeds of 3 up to 19 m s^{-1} for hundreds of kilometres. These flows represent a significant geohazard for submarine telecommunication cables and other seafloor infrastructure including that for the recovery of hydrocarbons (Carter et al., 2009; Parker et al., 2009). These submarine cables now carry >95% of global

data and communication traffic, giving them considerable strategic importance. Large submarine landslides also have the potential to generate damaging tsunami (Tappin et al., 2001; Haflidason et al., 2005; Boe et al., 2007; Tappin et al., 2014). Determining the frequency and triggers of these mass movements is key to submarine geohazard assessment.

A number of possible triggering mechanisms have been identified for submarine mass movements. Earthquakes, storm and tsunami wave loads, rapid depositional loading, hyperpycnal flows, volcanism and gas hydrate dissociation have all been identified as possible triggers (Adams, 1990; Mulder et al., 2003; Shanmugam, 2008; Piper and Normark, 2009; Stigall and Dugan, 2010; Talling, 2014). Despite identifying multiple triggers, there have been few occasions when a precise trigger for an event has been identified. In most case studies where a triggering mechanism has been identified, the trigger was identified using cable breaks.

1.1. Previous studies using cable breaks

Numerous studies have used cable breaks to study individual submarine mass movements (Heezen, 1956; Heezen et al., 1964; Heezen and Johnson, 1969; Krause et al., 1970; Piper et al., 1999; Hsu et al.,

* Corresponding author.

E-mail address: ed.pope@noc.soton.ac.uk (E.L. Pope).

2008; Carter et al., 2012; Cattaneo et al., 2012; Su et al., 2012; Ratzov et al., 2015). Earthquakes, hurricanes and hyperpycnal flows have all been identified as triggering mechanisms for submarine mass movements using cable breaks. The classic example is the 1929 Grand Banks submarine landslide. This submarine landslide was triggered by a M_w 7.2 earthquake (Heezen and Ewing, 1952; Piper et al., 1999). More recently cable breaks identified multiple submarine landslides offshore Algeria triggered by the 2003 Boumerdès earthquake (Cattaneo et al., 2012), whilst multiple submarine flows were caused by the 2006 Pingtung earthquake offshore Taiwan (Carter et al., 2012). In these cases, geophysical and shallow cores have corroborated the cable break data showing cable breaks can be used as proxy for mass flow triggering. Submarine cable breaks were also used to identify the occurrence of turbidity currents offshore Oahu, Hawaii as a result of the passing of Hurricane Iwa (Dengler et al., 1984). The passing of Typhoon Morakot over Taiwan in 2006 did not generate a submarine mass movement itself; it did, however, generate an exceptional discharge from the Gaoping River which generated a hyperpycnal flow (Kao et al., 2010). This was followed a few days later by the main flow triggered by failure of the recently deposited sediment (Carter et al., 2012). Cable break studies have also provided us with unique insights into submarine mass movement dynamics. Sequential breaks in networks of cables have enabled turbidity current flow speeds to be calculated (Heezen and Ewing, 1952; Piper et al., 1999; Carter et al., 2012).

In spite of the insights afforded by breaks to submarine cable networks, no study has previously been able to analyse the frequency and triggering mechanisms of submarine mass movements globally. Here, for the first time we have access to a global compilation of cable breaks over 25 years. The compilation allows us to analyse precisely what triggers and does not trigger submarine mass movements globally and identify whether these triggers are regionally specific or act at the global scale.

1.2. Turbidite palaeoseismology

Earthquakes and their related hazards (tsunami, fire, etc) are predicted to claim >2.5 million lives during the 21st century (Holzer and Savage, 2013). Efforts to reduce losses use estimates of earthquake size and recurrence. To achieve this, palaeoseismology attempts to extend the earthquake record beyond the instrumental record. One method of extending the earthquake record is turbidite palaeoseismology (Adams, 1990; Gràcia et al., 2013). This approach relies on discriminating between the mechanisms, which trigger turbidity currents and the resulting deposits (Goldfinger, 2011; Gràcia et al., 2013). It is achieved by (1) establishing synchronous triggering of sediment gravity flows over large areas using correlation of core deposits (Adams, 1990; Beck et al., 2007; Goldfinger, 2011; Patton et al., 2013; Atwater et al., 2014), (2) identifying specific seismo-turbidite facies within core deposits (Nelson et al., 1995; Goldfinger et al., 2012; Talling, 2014), (3) confluence tests (Adams, 1990), and (4) linking onshore geological records with offshore core data (Nanayama et al., 2007). The methods for testing whether a turbidite is earthquake triggered are summarised in Table 1.

Robust reconstruction of earthquake histories requires (1) deposits to be precisely dated; (2) the sedimentary regime of the region to be well constrained; (3) the sedimentary record to be complete; and (4) knowledge of which magnitude earthquakes do and do not trigger sediment gravity flows (Atwater and Griggs, 2012; Sumner et al., 2013; Atwater et al., 2014). Of these requirements, understanding which magnitude earthquakes do (and do not) trigger submarine mass movements is of critical importance. Onshore, landslides triggered by earthquakes can be directly observed (Keefer, 1984). From observations onshore it is possible to link different earthquake magnitudes, distances from hypocentres and changes in local geology to mass movements (Keefer, 1984, 2002; Owen et al., 2008). In contrast, it is more problematic to identify the occurrence or extent of well-dated

Table 1

Methods for testing whether a turbidite is earthquake triggered.
After Talling (2014).

How do you know if a turbidite records earthquake triggering?	Comment
1. Confluence test: Same number of turbidites on upstream and downstream sides of confluence indicates synchronous wide-spread triggering. Origin of flow is too widespread for other triggers of synchronous turbidity currents, such as cyclones that can produce hurricane-force winds across distances of several hundred kilometres.	Number of turbidites can vary with height above channel flow as flow thickness is variable. It is difficult to precisely locate cores (e.g. at a consistent height above the channel floor) using ship-mounted coring methods.
2. Synchronous deposition of turbidites in multiple basins indicates widespread slope failure. Origin of flow is too widespread for other triggers of synchronous turbidity currents.	Uncertainties in dating 'synchronous' turbidites
3. Turbidite volume is much larger than that expected for other trigger mechanisms such as river floods.	Deposit volume is rarely precisely known. Note that flows may incorporate sediment and increase their volume, through conduit erosion. Processes other than earthquakes can have the potential to trigger large landslides.
4. Earthquake and turbidite timing is independently well known, as timing observed directly – or in the case of earthquakes – through reliable historical records.	Cable breaks or mooring data may be needed to date turbidity currents precisely, as other methods (e.g. ^{210}Pb or ^{137}Cs) profiles of 'recent' turbidites have greater uncertainties. Ideally, repeat coring or mapping of the seafloor is needed to establish timing of turbidite emplacement. 4 is generally more reliable than 1-to-3.
5. Multiple stacked fining upward sequences inferred to be characteristic of earthquake triggered turbidites, as failure occurs in many locations across a wide area.	The grading pattern is not strongly diagnostic as multiple fining upward sequences can also result from multi-stage slope failure, flow reflection, or pulsing hyperpycnal flows.

synchronous mass movements in the marine environment. Access to a global submarine cable fault dataset provides the first opportunity to attempt such a study offshore.

1.3. Aims

Two main questions are posed. First, which magnitude earthquakes do (and do not trigger) submarine mass movements that break cables and does this vary on a regional basis? Second, do other parameters such as local sediment supply need to be assessed as part of turbidite palaeoseismology rather than just ground shaking (e.g. earthquake magnitude/peak ground acceleration)?

2. Terminology

Throughout this study the term 'cable break' or 'break' is used. Here we use these terms to refer to clean breaks and other faults in the cables. Faults can result from damage to a fibre-optic cable casing that allows the ingress of seawater and shorting of the power supply and/or stretch the cable to a point where optical fibres are damaged (Burnett et al., 2013).

We use the term *submarine mass movement* to denote an overall flow event driven by the excess density of the sediment that it contains. *Submarine mass movements* can refer to *turbidity currents*, *debris flows*, *hyperpycnal flows*, *slumps* and *landslides*. Transformation may occur between these different flow types as the submarine mass movement evolves. For further information on terminology for different types of flow see Talling et al. (2012). We refer to *submarine mass movements* and later *mass flows* as the cable break database only donates that a

cable experienced a fault and the day that the fault was experienced. It does not denote the type of flow that caused the cable to break or the precise timing of the break (i.e. minute accuracy). We are therefore unable to apply methods that have been used previously to estimate flow velocity (Piper et al., 1999; Carter et al., 2012) or identify the specific type of flow which has broken each cable.

3. Data and methods

3.1. Cable break database

This study is based on non-public, aggregated data supplied by Global Marine Systems Limited (UK) on a non-disclosure basis. The database contains information on the location of each subsea cable when it was laid (Fig. 1). It includes any other installation information such as sea bed type and the duration the cable has been in service. Cable breaks within the database are identified and generally related to specific causes, i.e. seismic, trawling, anchor, etc. Each 'break' refers to a break or failure along a section of a specific cable. Each 'break' may therefore represent multiple breaks along a single section of cable. For example, it has previously been reported that cable SEA-ME 3 suffered 11 breaks as a result of the 21/05/2003 Boumerdès earthquake offshore Algeria (Cattaneo et al., 2012), but these appear as a single break within the database.

3.2. Earthquakes

3.2.1. Earthquake magnitudes

Earthquake records from 1989 to present were obtained from the USGS ANSS Comprehensive Earthquake Catalogue (ComCat; <http://earthquake.usgs.gov/earthquakes/search/>). The catalogue provides

location, timing, type of earthquake, hypocentre depth, magnitude and magnitude type of each earthquake. Three types of magnitude are presented; surface wave magnitude (M_s), body wave magnitude (M_b) and moment magnitude (M_w). However, in order to assess the relationship between earthquake magnitude, ground shaking and submarine cable breaks, required earthquake magnitudes in the catalogue to be homogenised. To achieve this, M_s and M_b were converted to M_w using empirical relationships (Scordilis, 2006; Das et al., 2011; Di Giacomo et al., 2015).

3.2.2. Earthquake peak ground acceleration

In sub-aerial settings, earthquake M_w is not directly related to the number or size of co-seismic landslides that occur (Makdisi and Seed, 1977; Ambraseys et al., 1996; Meunier et al., 2007). Instead the number of landslides correlates well with the intensity and duration of seismic acceleration (Makdisi and Seed, 1977). The intensity and duration of seismic acceleration can vary from site to site for a given earthquake. Generally ground-shaking gets weaker with increasing distance from the ruptured fault that produced the seismic energy but it is also a function of local ground conditions, fault type and focus depth. A similar relationship may exist for submarine slope failures (Strasser et al., 2006; Noda et al., 2008; Pouderoux et al., 2014). Initiation of underwater slope failure may depend on excess pore pressure generated by earthquake induced shaking and other preconditioning factors such as slope architecture and mechanical properties of the sediment (Seed and Idriss, 1971; ten Brink et al., 2014). It is therefore necessary to compare ground shaking as well as magnitude to breaks in the subsea cable network. Only then are we able to evaluate earthquake triggering of submarine mass movements that break cables.

As part of the ComCat database the USGS also produces ShakeMaps for specific earthquakes. These maps provide estimates of ground

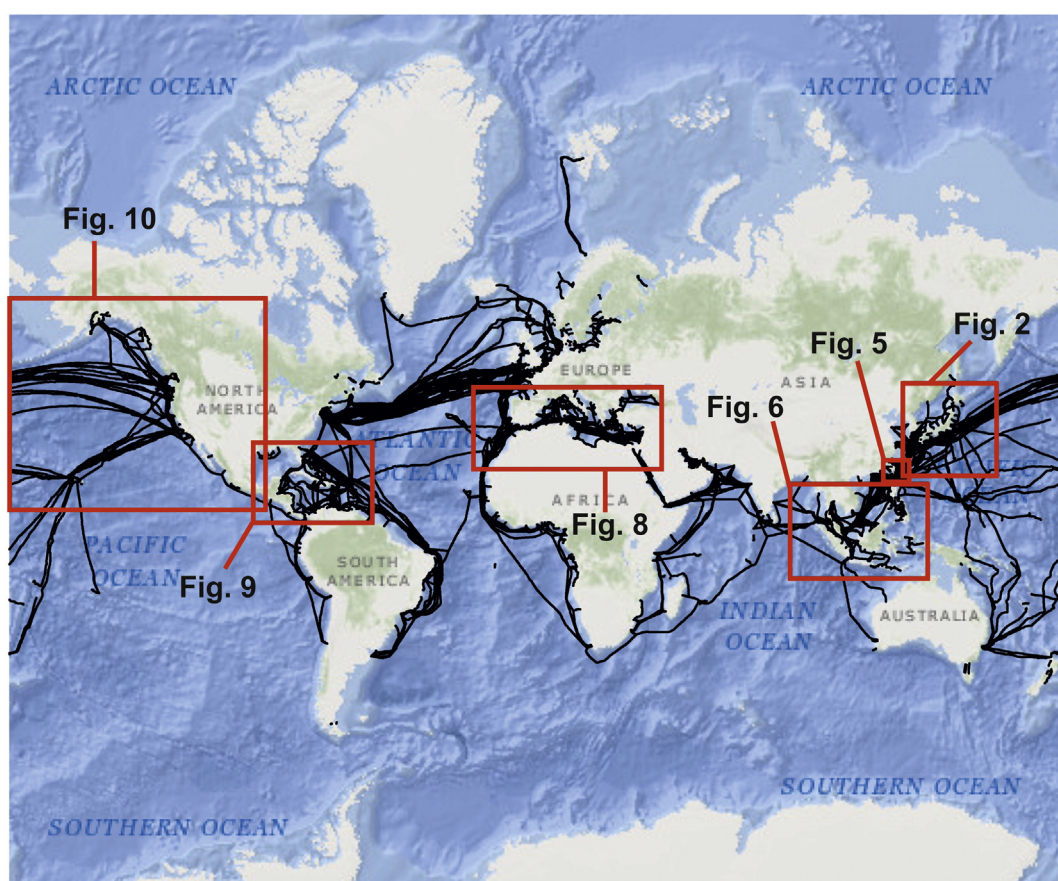


Fig. 1. Global submarine communication network with each study area identified.

shaking at sites depending on distance from the earthquake, the rock and soil conditions at each site and variations in the propagation of seismic waves from the earthquake resulting from complexities in the structure of the Earth's crust (Wald et al., 1999, 2005; Boore and Atkinson, 2008; Allen et al., 2009). These maps have a number of inherent uncertainties (Wald et al., 2008). Uncertainty at any point is dominated by (1) the influence of any proximal ground motion observations, and (2) estimation of ground motions from ground motion prediction equations. These uncertainties on land are compounded offshore as ground motion observations are usually unavailable. ShakeMaps are also only available for a small number of earthquakes. An independent method of producing estimates of Peak Ground Acceleration (PGA) for all the earthquakes in this study was therefore needed. This was achieved using the following empirical relationship (Si and Midorikawa, 1999).

$$\log A = b - \log(X + c) - kX \quad (1)$$

where A is PGA and X is fault distance in km set to 50 km. The coefficient k is fixed at 0.003. The terms b and c are calculated using the following relationships.

$$b = aM_w + hD + \sum d_i S_i + e + \varepsilon \quad (2)$$

$$c = 0.0055 \times 10^{0.50 M_w} \quad (3)$$

where D is the hypocentre depth (km), S_i is fault type, ε is a standard deviation. a , h , d , and e , are regression coefficients (see Si and Midorikawa, 1999 for more detail). Analysis of which earthquake PGAs did and did not trigger mass flows requires the location of mass flow initiation to be known. The cable break database, however, only provides a location for a break and not an initiation location. A fault distance of 50 km at which to calculate PGA was therefore arbitrarily chosen to enable comparison of earthquake PGAs and triggering of mass flows. These calculations therefore represent a simplified quantification of ground shaking and not a precise calculation of local shaking at the point of mass flow initiation (for a full discussion see Section 5.1).

3.3. How cable break and earthquake databases were compared

3.3.1. Earthquakes which triggered submarine mass movements

The cable break database was divided into different regions. Regions were chosen on the basis of similar seismic, sedimentary and climatic regimes. By analysing specific regions we can determine whether specific earthquake M_w can trigger submarine mass movements in each environmental setting. The regions are: (1) the Japanese Archipelago and the Korean Peninsula, (2) Taiwan, (3) Indonesia, Malaysia and the Philippines, (4) the Mediterranean, (5) the Caribbean, and (6) Pacific North America. We included all cable breaks in the dataset identified as having a seismic, landslide, chafe under current action, and other natural causes. Among these categories, cable breaks with a known cause unrelated to an earthquake were removed, e.g. shark bites. An earthquake was attributed to have caused a submarine mass movement if the cable break and the earthquake date were coincident, or within 24 h of one another. The 24 h threshold was set for an individual earthquake triggering a submarine mass movement as the database contained only the date and not the specific time of the break.

For each cable break we also analysed the earthquake record up to seven days before an actual break occurred. Longer seismic records were assessed to determine whether earthquake swarms could be linked to cable breaks instead of individual earthquakes. In this study a swarm is defined as multiple small ($< M_w 5.5$) earthquakes occurring across a limited area in a short period of time, i.e. less than 7 days. If an earthquake swarm was identified as the possible triggering mechanism for the cable break, the break was not considered in the main analysis. This was because we were unable to identify precisely which earthquake triggered the mass movement. The actual cause of the eventual failure may

also have been repeated seismic loading rather than the final seismic acceleration of the earthquake attributed as the trigger.

3.3.2. Earthquakes which did not trigger submarine mass movements

All earthquakes that failed to trigger a cable break were also collated. Earthquakes were collated from ComCat using the installation and decommission dates for cables presented in the cable database. Not all of these earthquakes are displayed in the subsequent analysis. For each region only earthquakes of a specific M_w are included. The M_w of earthquakes displayed reflects the seismicity of each region, i.e. earthquakes with lower magnitudes are included in the Caribbean than are included in Japan. This decision was made due to the extremely high number of low magnitude earthquakes, which affect some regions without breaking cables.

3.3.3. Cable breaks prior to 1989

Cable breaks caused by earthquakes and associated submarine mass movements have been reported before the period of observation of the cable break database in this study, e.g. Heezen and Ewing (1952). These are not considered in this paper. The benefit of the cable break database used in this study is that we can observe when subsea cables survive seismic events. We do not have information regarding when cables were not broken in historical subsea cable networks. We would therefore bias our analysis in favour of earthquakes triggering submarine mass movements if this historical data were included within our analysis.

4. Results

The results section is broken up into the different regions. For each region the number of cable breaks caused by earthquakes and their magnitudes (M_w) are reported. We also show how many earthquakes of a given M_w occurred whilst cables remained operational according to the seismicity of each region. This is because smaller magnitude earthquakes are only associated with cable breaks in a few locations.

4.1. Japan

Between January 1990 and January 2015 there were 18 cable breaks attributed to earthquakes off Japan (see Fig. 2a). These breaks occurred in water depths of between 2596 m and 6945 m. During this period there was a total of 230 earthquakes $\geq M_w 6.0$. The 18 cable breaks were associated to only 4 earthquakes with M_w ranging from $M_w 7.2$ to $M_w 9.0$. No cable breaks occurred in either the Sea of Japan or offshore Kyushu between 1990 and 2015. Earthquake swarms failed to cause cable-damaging mass flows.

The largest earthquake is the March 2011, $M_w 9.0$ Tohoku-oki earthquake, which caused 15 of the cable breaks. The earthquake had a PGA $> 25 \text{ m s}^{-1}$ (Fig. 3a). The submarine slope failure(s) triggered by the Tohoku-oki earthquake therefore were more extensive than the failures caused by the lower M_w events (Fig. 4). The cable breaks all occurred at the southern end of a major fault rupture in the Japan Trench, in a zone south of the submarine slumps proposed by Strasser et al. (2013) and Tappin et al. (2014). Strasser et al. (2013) contend that the observed slump did not contribute significantly to the Tohoku-oki tsunami whilst Tappin et al. (2014) suggest that the high run-up of the tsunami can only be explained by a submarine mass failure east of central Sanriku coast. No evidence of the mass flows are present in the cable break dataset as they occurred westward of the submarine cables running parallel to the Japanese coastline (see Figs. 2 and 4). We have no evidence of major mass flows, large enough to rupture cables, triggered along the central or northern areas of the fault rupture.

4.2. Taiwan

Between January 1993 and January 2015 there were 71 cable breaks associated with earthquakes around Taiwan (Fig. 5). These occurred in

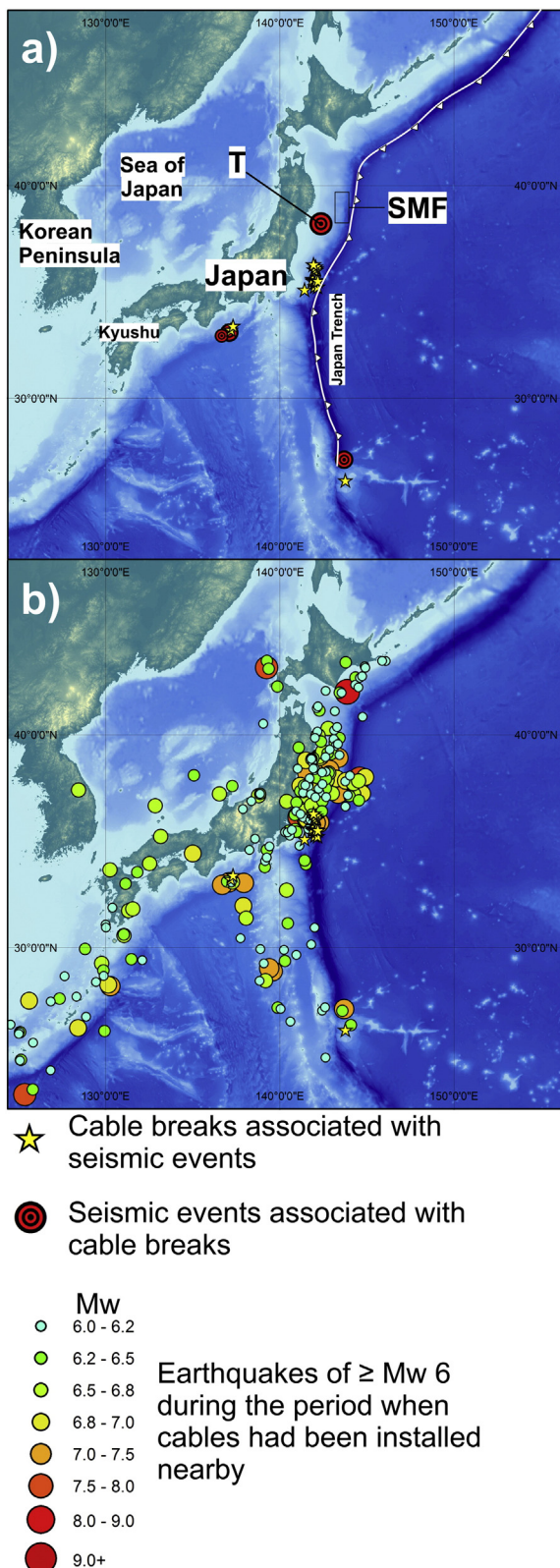


Fig. 2. Locations of submarine cable breaks and earthquakes around Japan and the Korean Peninsula. a) Locations of submarine cable breaks (yellow stars) and the epicentres of seismic events regarded to have triggered mass flows resulting in cable breaks. Diameter of earthquake epicentres reflects the M_w of the earthquake. b) Cable breaks (yellow stars) and the epicentres of all earthquakes $\geq M_w 6$ which occurred during the operational period of nearby cables. T = epicentre of the Tohoku-oki Earthquake. SMF = region where sediment mass failures caused by the Tohoku-oki earthquake have been thought to occur (Strasser et al., 2013; Tappin et al., 2014) (For interpretation of the references to colour in this figure legend, the reader is referred to the web version of this article.)

water depths of between 50 m and 6320 m. During this period there were 445 earthquakes $\geq M_w 5.0$. The 71 cable breaks are related to 37 earthquakes. Earthquake M_w which triggered mass flows ranged from $M_w 3.0$ to $M_w 7.1$. There is no apparent threshold of PGA for triggering mass flows around Taiwan (Fig. 3b). There were no cable breaks off western Taiwan directly related to earthquakes. This is likely a consequence of the sparseness of the cable network in this area, burial of cables beneath the seabed to protect them from fishing activities and the near-flat topography of the continental shelf and seabed. In addition to the 71 cable breaks attributable to individual earthquakes there are also 10 cable breaks that may be attributed to earthquake swarms.

4.3. Indonesia, Malaysia and the Philippines

Between January 1997 and January 2015 there were 7 cable breaks potentially caused by earthquakes in the region (Fig. 6). These cable breaks occurred in water depths of between 1000 m and 2340 m. During the period of observation there were 72 earthquakes $\geq M_w 6.0$, 5 of which ($M_w 6.0$ to $M_w 9.2$) caused the cable breaks. One cable break was attributed to an earthquake swarm.

The greatest earthquake recorded in this region, and the largest in the database was the $M_w 9.2$ 26/12/2004 Boxing Day earthquake. The earthquake caused three cable breaks near the Andaman and Nicobar Islands (Figs. 6a and 7) but did not break all the cables in these areas. Three cables run between the Andaman and Nicobar Islands and perpendicular to the subduction trench. Here, only one of the cables was broken. Three subsea cables run between Sumatra and the Nicobar Islands perpendicular to the trench. Here, two of the cables were broken. The earthquake therefore resulted in flows which broke only 50% of the cables in the area.

4.4. Mediterranean

Between January 1989 and January 2015 there were 8 cable breaks, which could be attributed to earthquakes in the Mediterranean Sea and Atlantic Ocean off Morocco and Spain (Fig. 8). These cable breaks occurred in water depths of between 398 m and 2739 m. During the period of observation there were 208 earthquakes $\geq M_w 5.0$. The 8 cable breaks are attributed to 4 earthquakes from $M_w 5.1$ to $M_w 7.6$. The strongest of these was the Izmit Earthquake in Turkey on 17/08/1999, which caused mass flows in the Marmara Sea (Tinti et al., 2006). This was the only $> M_w 7.0$ event during the study period. No cable breaks were reported for the same period in the eastern Mediterranean despite its relatively higher seismicity compared with the rest of the Mediterranean.

The largest number of cable breaks occurred in the central Mediterranean as a consequence of the 2003 Boumerdès earthquake. It was responsible for 28 cable breaks (Cattaneo et al., 2012). In our database this earthquake caused 5 cable breaks. The discrepancy between studies is a consequence of multiple breaks to the same cable being presented as one cable break in our database. This large number is a consequence of the cable orientation which is parallel with the continental margin – the site of multiple landslides in the area. Two additional cable breaks occurred offshore Algeria in a similar location to the Boumerdès earthquake breaks (Dan et al., 2009; Cattaneo et al., 2012; Ratzov et al., 2015). These are probably the result of subsequent earthquake swarms.

4.5. Caribbean

From January 1995 to January 2015 there were 5 cable breaks probably caused by earthquakes (Fig. 9). These breaks occurred in water depths between 558 m and 2150 m. During the period there were 170 earthquakes $\geq M_w 5.0$. The 5 cable breaks are attributed to 4 seismic events with magnitudes of $M_w 3.1$ to $M_w 7.3$. Every earthquake with a $PGA > 2.5 \text{ ms}^{-2}$ triggered a mass flow. There were no cable breaks caused by earthquake swarms.

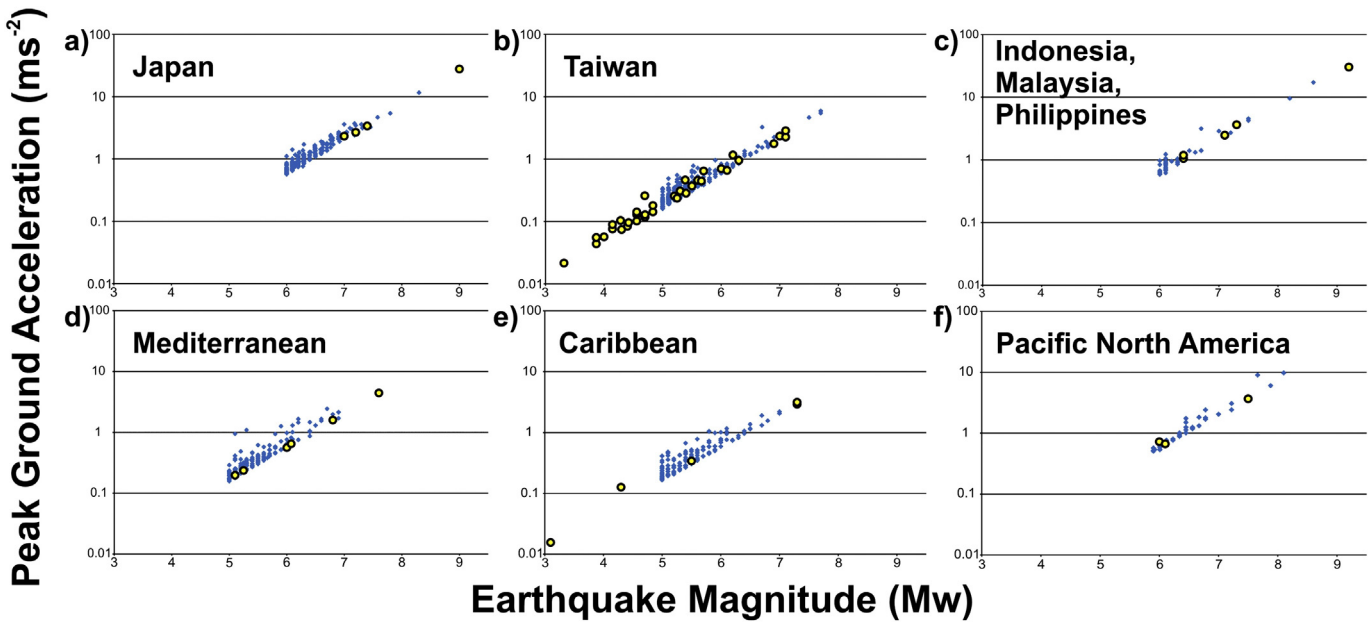


Fig. 3. Relationship between peak ground acceleration (PGA) felt 50 km away from the epicentre and magnitude (M_w). Blue diamonds indicate earthquakes, which are *not* associated with cable breaks. Yellow circles with black borders indicate earthquakes, which *are* associated with cable breaks. a) Earthquakes in Fig. 2b. b) Earthquakes in Fig. 5b. c) Earthquakes in Fig. 6b. d) Earthquakes in Fig. 8b. e) Earthquakes in Fig. 9b. f) Earthquakes in Fig. 10b. (For interpretation of the references to colour in this figure legend, the reader is referred to the web version of this article.)

4.6. Pacific North America

From January 1995 to January 2015 there were 5 cable breaks, which could be attributed to earthquakes in Pacific North America (Fig. 10). Breaks occurred in water depths of 171 m to 3220 m. During the period of observation there were 46 earthquakes of $\geq M_w 6.0$. All breaks are attributed to 3 earthquakes with magnitudes ranging from $M_w 3.2$ to M_w

7.5. The greatest M_w earthquake, $M_w 8.0$ (09/10/1995), was not associated with a cable break. No cable breaks resulted from earthquake swarms.

4.7. Global analysis

In the database there were 113 separate cable breaks caused by individual earthquakes and 13 caused by earthquake swarms. Most breaks

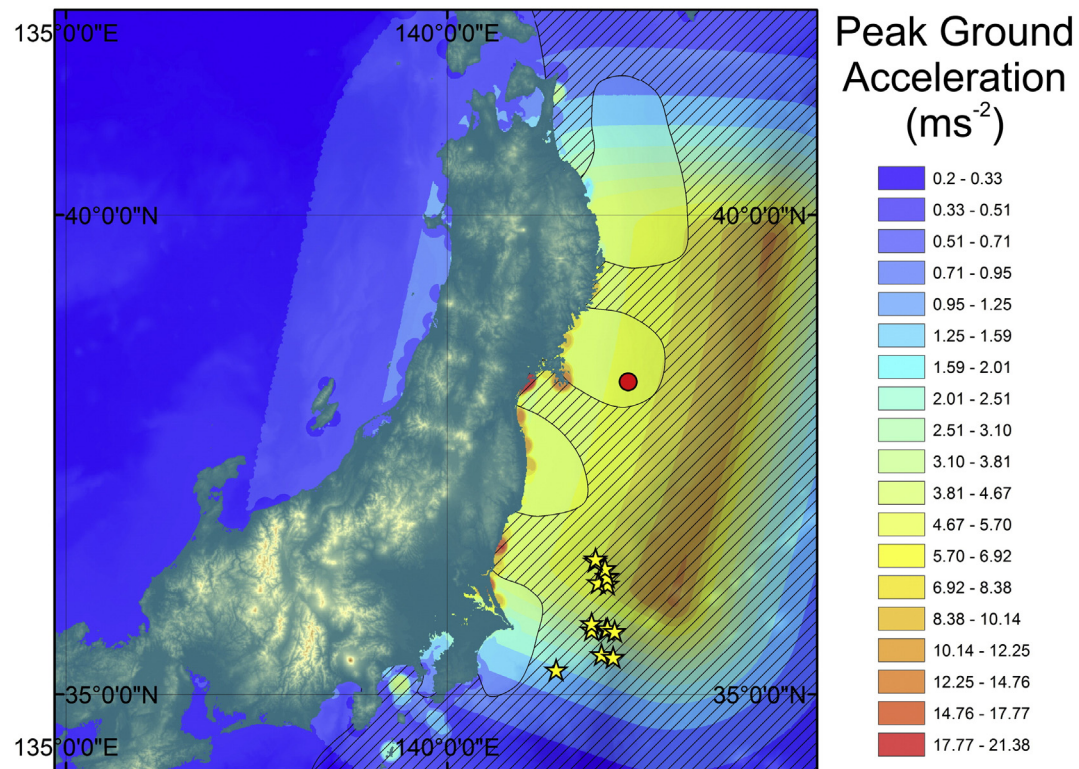
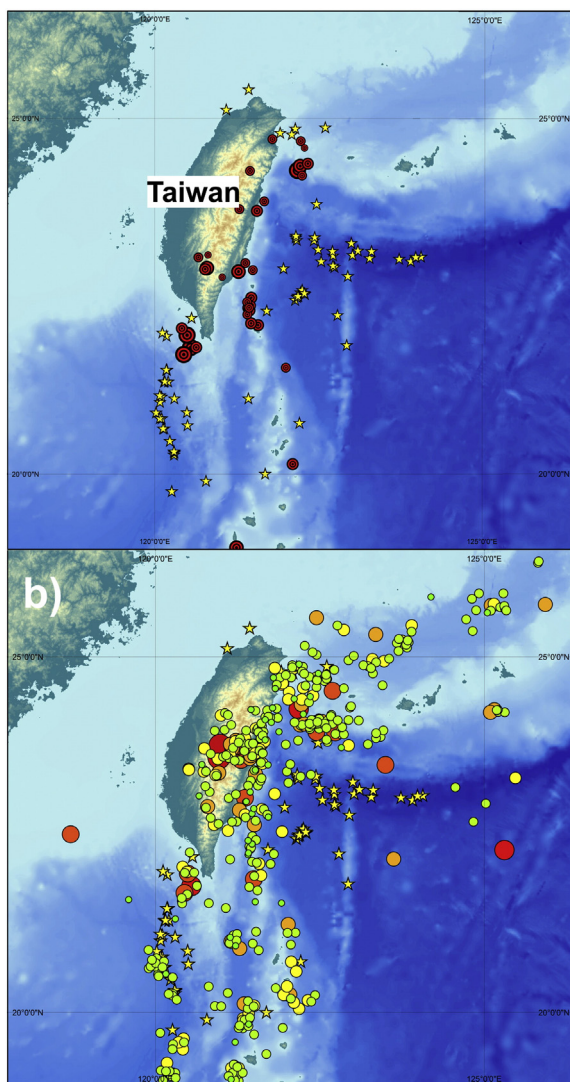


Fig. 4. ShakeMap generated by the USGS for the Tohoku-oki 2011 earthquake. Shows Japan with known submarine cable breaks denoted by yellow stars. Black dashed line represents the fault rupture zone (Ide et al., 2011). Red dot represents earthquake epicentre. Areas covered with cables represented by hatch shading. (For interpretation of the references to colour in this figure legend, the reader is referred to the web version of this article.)

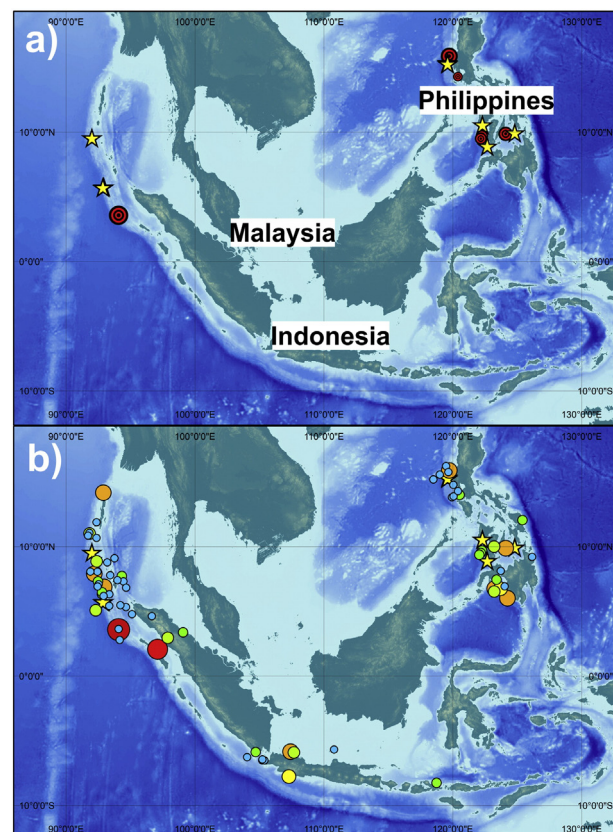


★ Cable breaks associated with seismic events
● Seismic events associated with cable breaks

- Mw**
- 4.5 - 5.0 Earthquakes of $\geq M_w 4.5$ during the period when cables had been installed nearby
 - 5.0 - 5.5
 - 5.5 - 6.0
 - 6.0 - 6.5
 - 6.5 - 7.0
 - 7.0 - 7.5
 - 7.5 - 8.0

Fig. 5. Locations of cable breaks and earthquakes around Taiwan. a) Locations of submarine cable breaks (yellow stars) and the epicentres of seismic events regarded to have triggered mass flows resulting in cable breaks. Diameter of earthquake epicentres reflects the M_w . b) Cable breaks (yellow stars) and the epicentres of all earthquakes $\geq M_w 4.5$, which occurred during the operational period of nearby cables. (For interpretation of the references to colour in this figure legend, the reader is referred to the web version of this article.)

were found around Taiwan (see Table 2) and reflects the high density of submarine cables, an exceptional fluvial discharge and the island's high seismicity (Milliman and Meade, 1983; Dadson et al., 2004; Kao et al.,



★ Cable breaks associated with seismic events

● Seismic events associated with cable breaks

M_w

- 6.0 - 6.2
- 6.2 - 6.5
- 6.5 - 6.8
- 6.8 - 7.0
- 7.0 - 7.5
- 7.5 - 8.0
- 8.0 - 9.0
- 9.0+

Earthquakes of $\geq M_w 6$ during the period when cables had been installed nearby

Fig. 6. Locations of cable breaks and earthquakes around Indonesia, Malaysia and the Philippines. a) Locations of submarine cable breaks (yellow stars) and the epicentres of seismic events regarded to have triggered mass flows resulting in cable breaks. Diameter of earthquake epicentres reflects the M_w of the earthquake. b) Cable breaks (yellow stars) and the epicentres of all earthquakes $\geq M_w 6$, which occurred during the operational period of nearby cables. (For interpretation of the references to colour in this figure legend, the reader is referred to the web version of this article.)

2010; Su et al., 2012; Liu et al., 2013). Globally there was no apparent threshold of earthquake M_w for causing mass flows. Fig. 11 shows the 2 recorded $\geq M_w 9.0$ earthquakes triggered mass flows, but that none of the $M_w 8.0-8.9$ events caused mass flows. The sample size of $M_w 9.0$ earthquakes ($N = 2$) prevents any robust conclusions regarding their triggering potential. Fig. 11 also indicates that the number of earthquakes, which triggered mass flows increases with the frequency of earthquakes of that given M_w . However, the number of earthquakes of a given M_w does not directly relate to the number of flows triggered. With the exception of the two $\geq M_w 9.0$ events, the cable break database does not indicate a globally consistent threshold magnitude and PGA that systematically produce mass flows.

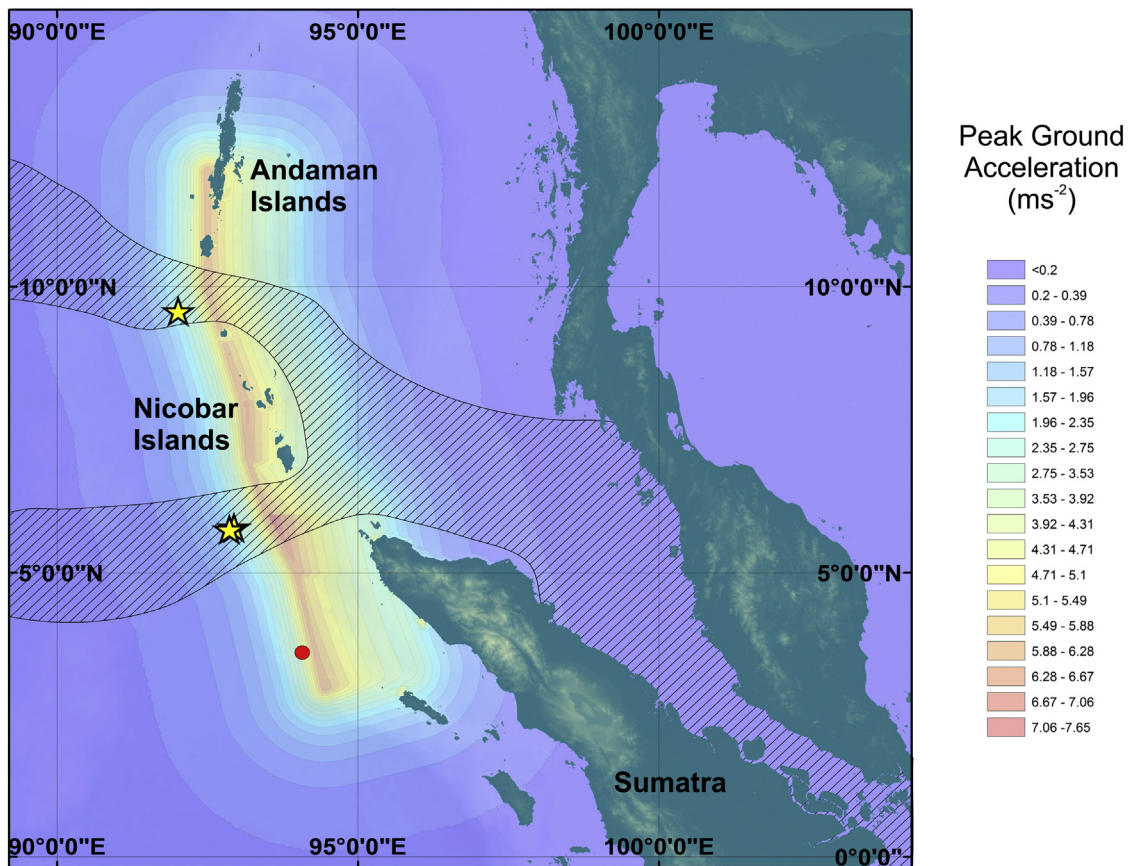


Fig. 7. ShakeMap generated by the USGS for the Boxing Day 2004 earthquake. Sumatra, the Nicobar and Andaman Islands, and Thailand are shown with submarine cable breaks denoted by yellow stars. Red dot represents earthquake epicentre. Hatch shading denotes the areas covered by submarine cables. (For interpretation of the references to colour in this figure legend, the reader is referred to the web version of this article.)

5. Discussion

5.1. Uncertainty within the cable break analysis

Access to the cable break database is extremely valuable for identifying which earthquakes trigger, and do not trigger, submarine mass movements. However, a number of the following points should be noted. First, in most cases the coincidence of cable breaks with earthquakes is compelling. However, we cannot say with absolute confidence that each submarine mass movement was triggered by the earthquake itself, or if other triggering mechanisms also occurred on the same day as the earthquake. Such a coincidence is, however, relatively unlikely. It is also possible that the submarine mass movement occurred independently of the earthquake which we have identified as being the triggering mechanism.

Second, the cable break database is a record of where a submarine mass movement has broken a cable. It does not indicate the location of the initial failure of the seafloor. We have therefore been unable to calculate a PGA for the mass failure initiation location. Nor is it appropriate to calculate the PGA at the cable break location as flows are capable of running out 100s of kilometres. The decision was therefore made to choose an arbitrary distance from the epicentre of each earthquake, namely 50 km, in order to calculate comparable PGAs for each earthquake (Campbell, 1997, 2003). It must, however, be recognised that this represents a simplification of a complex processes. A large magnitude (>8 M_w) will result in a large rupture zone compared to a small magnitude earthquake. The area that will therefore be affected by the highest PGA values for a given earthquake will be highly variable (Wells and

Coppersmith, 1994). Our analysis simplifies these differences meaning that there remains a large uncertainty with regards to the relationship of the area of the seafloor impacted by high intensity seismic shaking and the initiation of mass flows.

Third, the cable break database may not represent every submarine mass movement. To break a cable, the flow has to impart sufficient force to physically stretch and break the cable, or abrade the casing. The required force to achieve this varies according to flow type (see Section 2), cable type (armoured, not armoured, etc), the age of the cable, orientation to the mass flow and the amount of slack or whether the flow buries the cable rather than breaks it. Even where flows have been sufficiently powerful to break a cable, it has been shown that it may not break all adjacent cables (Hsu et al., 2008; Carter et al., 2012). If a flow fails to break a cable it will not be registered. A limitation of cable break techniques used to detect flows is that they are partly controlled by the distribution of cables. Globally, the ocean coverage by cables is uneven (see Fig. 1). Areas such as Taiwan have a high density of cables compared to other regions such as the Eastern Pacific. The combination of these factors means that it is more likely that submarine mass movements will be identified in areas with high cable densities. Thus flows may not be captured where cables are sparse, such as off South America (Fig. 1).

A number of examples of where mass flows are known to have occurred but have not been detected by the cable break database exist. First, the Haiti earthquake on 12/01/2010 did not produce a mass flow according to the cable break database, as no cables were broken. However, McHugh et al. (2011) report core evidence of a turbidite derived from the earthquake. The location of the cores and the local bathymetry

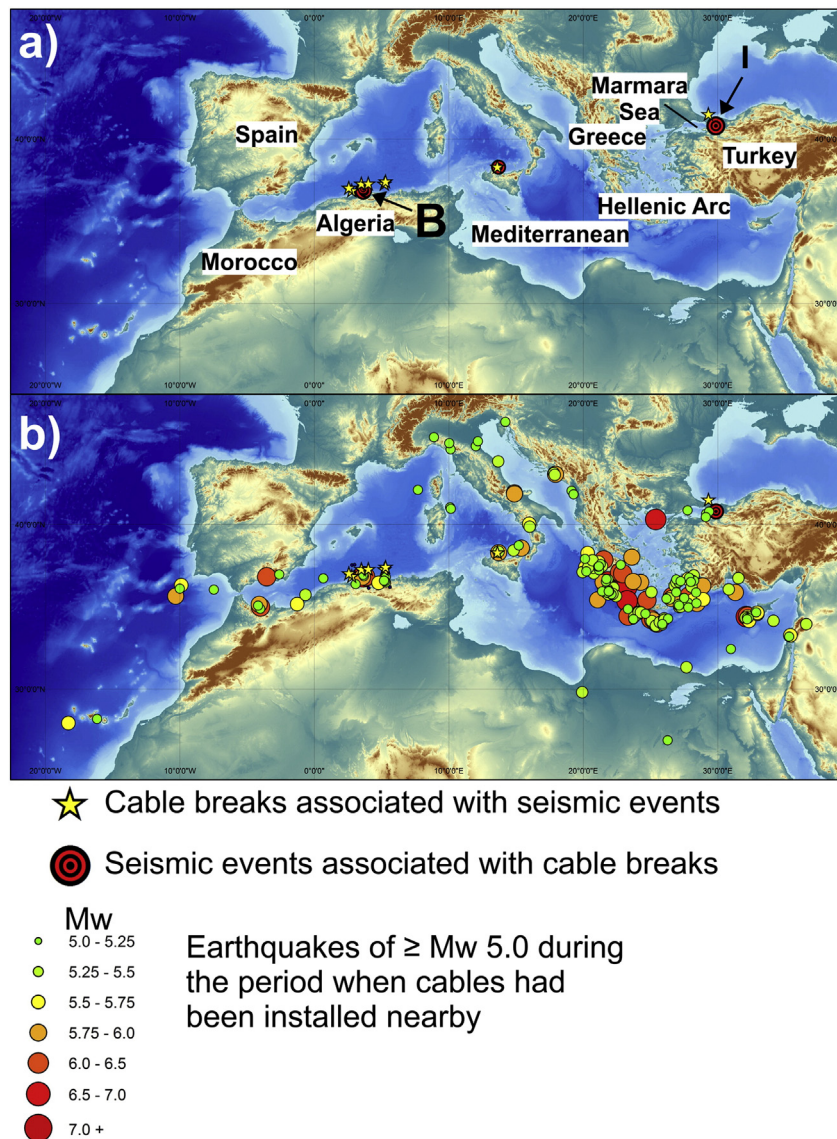


Fig. 8. Locations of cable breaks and earthquakes around the Mediterranean. a) Locations of submarine cable breaks (yellow stars) and the epicentres of seismic events regarded to have triggered mass flows resulting in cable breaks. Diameter of earthquake epicentres reflects the M_w of the earthquake. b) Cable breaks (yellow stars) and the epicentres of all earthquakes $\geq M_w 5$, which occurred during the operational period of nearby cables. Note B = 2003 Boumerdès epicentre; I = 1999 Izmit epicentre. (For interpretation of the references to colour in this figure legend, the reader is referred to the web version of this article.)

suggest that the cable in the area was not affected by the flow. They suggest that from its initial triggering location, the bathymetry would have interacted with the flow resulting in it being diverted away from the cable. Second, turbidity currents appear to have been triggered by earthquakes in the Cariaco Basin, Venezuela (Lorenzoni et al., 2012). An active cable is present across the basin but was not broken. Possible explanations for this are (1) a turbidity current was triggered but it was of insufficient strength to break the cable; (2) the cable was protected by local bathymetry or was buried by the turbidity current; or (3) the increased backscatter which was recorded by optical instruments in the basin was actually measuring an increase in river suspended sediment as a result of the earthquake but not a turbidity current. Unfortunately, the correct scenario remains as yet unclear.

Fourth, not all cable breaks worldwide during the study period are recorded in the database. The database is a compilation of breaks repaired by Global Marine Systems Ltd. together with other breaks reported by clients and collaborators. There may, however, be cable breaks that are unreported.

5.2. Which magnitude earthquakes do and do not trigger submarine mass movements?

5.2.1. Is there an earthquake magnitude that will systematically trigger a mass flow?

It is well known that earthquakes trigger sub-aerial landslides (Keefer, 1984). The minimum earthquake magnitude often cited to trigger a sub-aerial landslide is $\sim M_w 5.0$ (Keefer, 1984, 2002). In submarine environments earthquakes of $> M_w 5.0$ have been suggested to cause small volume failures (Niemi and Ben-Avraham, 1994; Piper et al., 1999; Lorenzoni et al., 2012; Patton et al., 2013). Magnitudes $> M_w 7.0$ have been cited as the minimum required for the generation of a turbidity current through the triggering of a submarine landslide (Nakajima and Kanai, 2000; Goldfinger et al., 2003; Poulderou et al., 2012; Moernaut et al., 2014). The cable break database does not, however, demonstrate that earthquakes $> M_w 7.0$ will necessarily generate submarine mass movements, or at least mass flows sufficiently powerful to cause cable breaks. In every region, except the Mediterranean (see

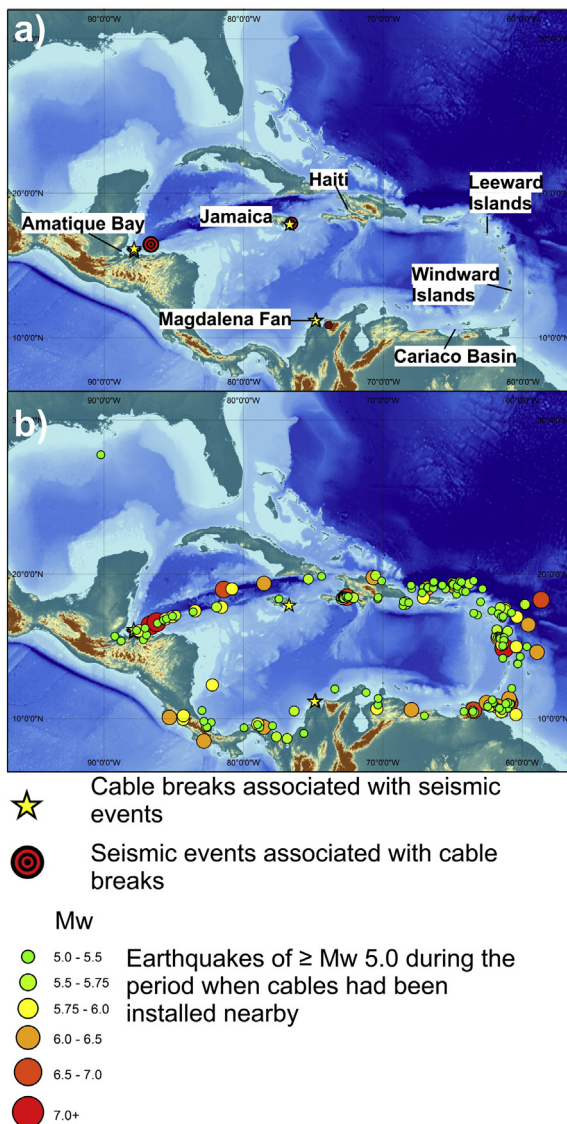


Fig. 9. Locations of cable breaks and earthquakes around the Caribbean. a) Locations of submarine cable breaks (yellow stars) and the epicentres of seismic events regarded to have triggered mass flows resulting in cable breaks. Diameter of earthquake epicentres reflects the M_w of the earthquake. b) Cable breaks (yellow stars) and the epicentres of all earthquakes $\geq M_w 5.0$, which occurred during the operational period of nearby cables. (For interpretation of the references to colour in this figure legend, the reader is referred to the web version of this article.)

Figs. 3d and 8b), there are $>M_w 7.0$ earthquakes that failed to generate mass flows with sufficient force to break a cable (Fig. 3).

In the regions considered in this study there were 365 earthquakes between $M_w 6.0$ and $M_w 7.0$; 43 earthquakes between $M_w 7.0$ and $M_w 8.0$; 4 between $M_w 8.0$ and $M_w 9.0$ and 2 $\geq M_w 9$. The proportions of these earthquakes which did and did not trigger flows are outlined in Table 2.

If we consider PGA rather than M_w as the factor affecting mass flow formation, a similar relationship can be seen (Fig. 3). Both $M_w \geq 9$ earthquakes generated mass flows which broke cables. These earthquakes had PGAs $>25 \text{ m s}^{-2}$. The PGAs of the 4 $M_w 8.0$ earthquakes varied between 8.5 and 17 m s^{-2} , yet no mass flows were generated. These PGA values all exceed the threshold for slope failure and turbidity current generation as proposed for the Hikurangi Margin, New Zealand (Pouderoux et al., 2014), the Eel Margin, California (Lee et al., 1999), the Aegean Trough, Mediterranean Sea (Lykousis et al., 2002) and the Southern Kuril Trench, North Pacific Ocean (Noda et al., 2008). Considering the PGA values of earthquakes $< M_w 8.0$, there is no simple



Fig. 10. Locations of cable breaks and earthquakes around Pacific North America. a) Locations of submarine cable breaks (yellow stars) and the epicentres of seismic events thought to have triggered mass flows resulting in cable breaks. Diameter of earthquake epicentres reflects the M_w of the earthquake. b) Cable breaks (yellow stars) and the epicentres of all earthquakes $\geq M_w 6$ which occurred during the operational period of nearby cables. (For interpretation of the references to colour in this figure legend, the reader is referred to the web version of this article.)

relationship between earthquakes which do, and do not, trigger mass flows according to the cable break database. Worldwide, increasing PGA, increases the probability that a submarine mass failure will occur, but it does not necessitate one.

Table 2

Counts of earthquakes which trigger mass flows which broke cables and earthquakes which did not trigger mass flows that broke cables. Counts for each region are stated as well as the total counts of all regions.

Region	M _w range	Triggered mass flow that broke cable	Did not triggered mass flow that broke cable	Percentage of earthquakes which triggered a mass flow
Global	6–7	13	350	4
	7–8	13	37	26
	8–9	0	4	0
	9+	2	0	100
Japan	6–7	0	176	0
	7–8	4	19	17
	8–9	0	1	0
	9+	1	0	100
Taiwan	5–6	12	330	4
	6–7	5	41	11
	7–8	3	3	50
	8–9	0	0	–
Indonesia, Malaysia and the Philippines	6–7	2	49	4
	7–8	2	5	28
	8–9	0	2	0
	9+	1	0	100
Mediterranean	5–6	1	167	100
	6–7	3	28	10
	7–8	1	0	100
	8–9	0	0	–
Caribbean	5–6	1	144	0.7
	6–7	0	22	0
	7–8	2	2	50
	8–9	0	0	–
Pacific North America	9+	0	0	–
	6–7	3	37	5
	7–8	1	6	14
	8–9	0	1	0
	9+	0	0	–

5.2.2. What is the minimum earthquake magnitude which can trigger a mass flow?

The minimum earthquake magnitude previously suggested to be capable of triggering a submarine mass movement is ~M_w 5.0. However, the cable break database contains information contrary to this assumption. Individual earthquakes with M_w as low as 3.1 are shown to have triggered mass flows in two locations (see Fig. 3). Whilst these may be rare (there are only 2 in the database) there are a large number of earthquakes with M_w between 4.0 and 5.0 which have caused cable breaking mass flows (15 events). In both cases, however, these represent only a very small proportion of the number of M_w 3.0–5.0 earthquakes which occur

globally ever year. These records indicate that certain conditions can arise on the seafloor where the release of small amounts of energy from low magnitude earthquakes can cause slope failures. From our analysis these conditions appear to be most prevalent around Taiwan (see Fig. 3).

5.2.3. Earthquake swarms

The cable break database contains 11 cable breaks which have been caused by mass flows triggered by earthquake swarms. The spatial characteristics of these events closely match those for mass flows triggered by individual earthquakes. The majority of earthquake swarm triggered flows (8) occurred offshore of Taiwan. The continental slopes in these

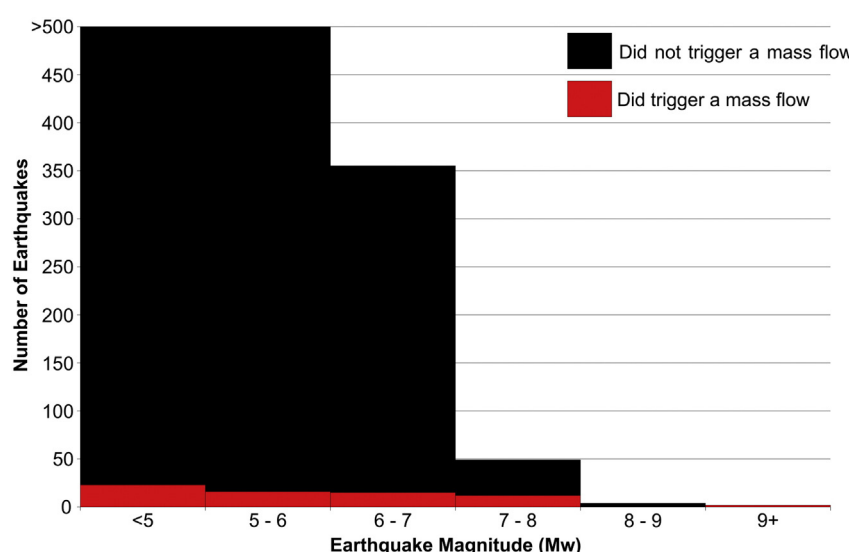


Fig. 11. Comparison of the number earthquakes which triggered mass flows which broke cables to those which did not trigger cable breaking mass flow events.

locations may therefore be more susceptible to failure resulting from seismic shaking as a consequence of local site characteristics (see subsequent discussion).

The two earthquake swarms which triggered mass flows in the Mediterranean occurred shortly after the 2003 Boumerdès earthquake, which itself triggered 5 cable breaks. These events add a further degree of complexity to understanding which earthquakes do (and do not) trigger flows. The flows triggered as a result of the earthquake swarms occurred within 2 months of the main earthquake and consequently there are two possible explanations for their triggering. First, the main earthquake preconditioned the slope to further failures. This could have been the result of either unloading as a consequence of the landslides triggered by the main earthquake or weakening of the substrate due to the shaking itself. Both scenarios facilitate slope failures to be triggered by further low intensity seismic shaking. Second, the large number of landslides caused by the main earthquake indicates that the continental slope in the region was susceptible to failures caused by seismic shaking. Therefore, the low intensity high frequency shaking associated with the earthquake swarms may have been sufficient to trigger mass flows. In either case, identification the different timing of the swarm related flows to the main earthquake triggered flows would be extremely difficult using only their deposits.

5.3. Is there a regional relationship between seismicity, sediment supply and mass flow occurrence?

Here we discuss the relationships observed between earthquake magnitude and cable breaks for the regions outlined in Section 4.

5.3.1. Japan

The Japan results support previous suggestions that submarine slope stability is greater in high magnitude seismic areas (Noda et al., 2008; Sumner et al., 2013). No earthquake $< M_w 7.0$ triggered a submarine mass movement in the Japanese region. This could either mean that there was no sediment suitable for mass flow formation or repeated ground shaking has resulted in consolidation and strengthening of seafloor sediments (Lee et al., 1993, 1996; Sultan et al., 2004; Vanoudheusden et al., 2004; Völker et al., 2011; Sumner

et al., 2013). Enhanced consolidation resulting from seismic shaking is made more likely by low sediment supply to the continental shelf in this region (Fig. 12). The low sediment supply prevents large accumulations of unstable sediment from developing. Thus the likelihood of weak seismic shaking causing a slope failure is greatly reduced resulting in the small number of triggered mass flows that we observe. Enhanced consolidation of seafloor sediment would also reduce the probability that large magnitude earthquakes will trigger mass flows; the cable break database suggests that out of 25 earthquakes with $\geq M_w 7.0$ only 5 of these actually triggered mass flows.

5.3.2. Taiwan

In contrast to Japan, earthquakes ranging from $M_w 3.7$ to $M_w 7.1$ triggered mass flows causing cable breaks off Taiwan. The magnitude range and the number of cable breaks, suggests that the continental slopes offshore Taiwan are inherently more unstable than other areas within this study as events are commonly triggered by very low M_w earthquakes. The preponderance of mass flows off Taiwan is likely due to local site characteristics.

A combination of active tectonism, steep topography, heavy rainfall and intense human activity results in sediment discharge from Taiwan of $180\text{--}380 \text{ Mt a}^{-1}$ (Dadson et al., 2004; Kao et al., 2010; Liu et al., 2013). This reflects an erosion rate 50 times more than the global average (see Fig. 12). A narrow eastern continental shelf, steep continental slope (Ramsey et al., 2006) and large volumes of poorly consolidated sediment that are replenished annually, collectively favour formation of seismically induced mass flows compared to almost any other location worldwide (Milliman and Meade, 1983; Milliman and Syvitski, 1992). Large numbers of cables also cross submarine canyons offshore Taiwan and lie perpendicular to the flow direction. The likelihood that they will be hit by a channelized flow sufficiently strong enough to break them is therefore increased.

Despite the favourable conditions for seismically triggered mass flow events, the three largest earthquakes ($M_w 7.0\text{--}8.0$) did not trigger mass flow events. It is remarkable that earthquakes which do not trigger mass flows can have PGAs two orders of magnitude greater than those that have triggered mass flows. It is also noteworthy that the 2006 $M_w 6.9$ Pingtung Earthquake ($M_L 7.0$) earthquake caused a turbidity current

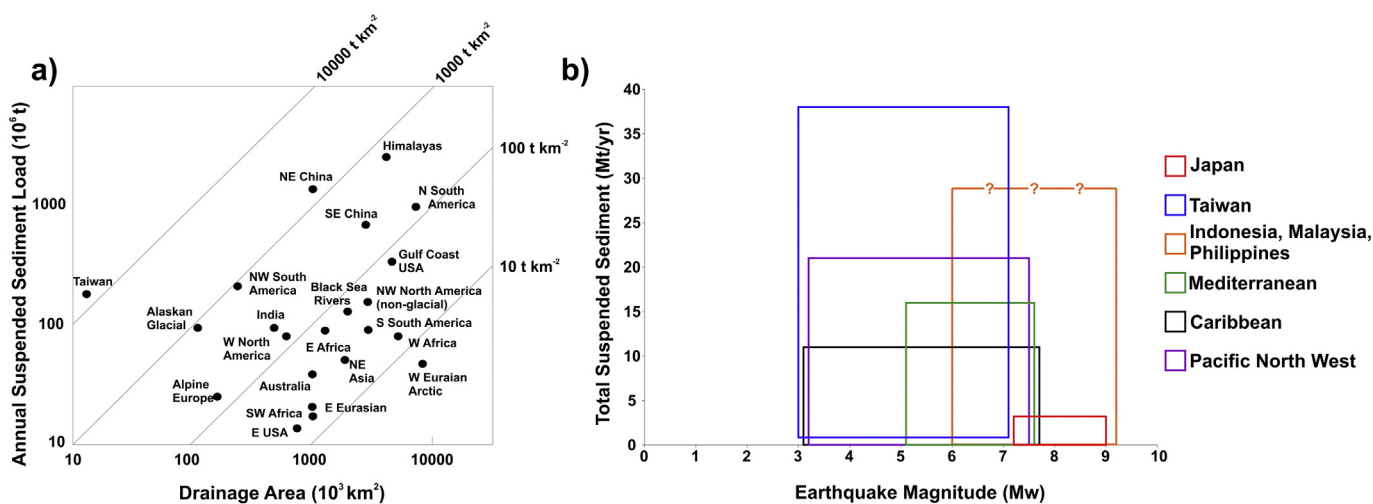


Fig. 12. a) Variations of annual suspended sediment load with drainage area (Milliman and Meade, 1983; Milliman and Farnsworth, 2011). Compared to the rest of the world, Taiwan is shown to be exceptional in terms of the volume of sediment generated when the drainage area of its rivers is taken into consideration. b) Range of estimated total suspended sediment discharged by major rivers within each study area where earthquakes have occurred against earthquake magnitudes known to trigger cable breaking flows. The volume of discharged sediment from Taiwan is shown to be exceptional. There is a large amount of uncertainty regarding the maximum amount of total suspended sediment discharged from rivers in Indonesia, Malaysia and the Philippines. This is a consequence of the lack of data for the majority of large rivers in the regions where earthquakes occur. Note that the total suspended sediment discharge data from the Magdalena River (140 Mt yr^{-1} ; Milliman and Farnsworth, 2011) has been omitted from the figure due to its exceptional nature compared to other rivers in the Caribbean region. There is also a lack of sediment discharge data from rivers on smaller Caribbean islands.

which broke 14 subsea cables and ran out >300 km, but larger earthquakes did not trigger similar flows. Understanding why very small earthquakes triggered mass flows whilst large earthquakes do not produce mass flow events is a crucial question with regards to understanding the triggering mechanisms of submarine flows.

5.3.3. Indonesia, Malaysia and the Philippines

Contrasts between the sedimentary regimes across the region are shown by their response to earthquake shaking. Only the M_w 9.2 Boxing Day Earthquake was able to trigger a mass flow event capable of breaking cables offshore of Sumatra, Java and the Andaman and Nicobar Islands. Neither M_w 8 earthquakes nor lower M_w earthquakes generated mass flows. Whilst the full impact of the Boxing Day event cannot be realised because of an absence of cables it appears that this area has a similar sediment consolidation regime to Japan. It is, however, difficult to directly compare the flow responses to the Boxing Day Earthquake and the Tohoku-oki Earthquake as a consequence of the contrasting cable coverages. Japan has at least 25 cables whilst Sumatra has about 5. This means that realistic comparisons can only be made through extensive sedimentary and geophysical surveys of both margins to identify mass flow deposits. It also means that the likelihood of detecting events from smaller earthquakes is much higher around Japan than Sumatra.

In contrast to Sumatra, around the Philippines, earthquakes between M_w 7.3 and M_w 6.4 triggered flow events. Lower magnitude earthquake swarms have also triggered mass flows. Like Taiwan, a large amount of sediment is discharged annually from the Philippines as a result of high annual precipitation, typhoons and readily eroded rock (Milliman and Meade, 1983; Milliman and Farnsworth, 2011). It is therefore unsurprising that all of the cable breaks are within 50 km of the shore and are associated with river mouths as large amounts of sediment is deposited annually in these locations. Compared to Taiwan, there are comparatively few breaks in this area which is likely a result of (1) the low density of the cable network; (2) the younger age of much of the cable network; (3) a lower seismicity regime than Taiwan and, (4) the limited number of cables which cross submarine canyons. It is likely therefore that more flows occurred in this region than have been documented.

5.3.4. Mediterranean

The seismic and sedimentary regimes of the Mediterranean are highly variable. The majority of earthquakes in the region occurred around Greece and the Hellenic Arc (Fig. 8). Previous studies have identified that despite the irregular, steep relief, active faults and high seismicity seen around Greece and the Hellenic Arc there are comparative few slope failures (Chronis et al., 2000; Camerlenghi et al., 2010; Strozyk et al., 2010). Few slope failures occur as a consequence of tectonically exhumed sediments being over-consolidated and bear high shear resistance and thus need a large earthquake to induce failure (McAdoo et al., 2000; McAdoo and Watts, 2004). Our results support these assertions suggesting similar processes to Japan and Sumatra.

5.3.5. Caribbean

The Caribbean shows large contrasts between different areas in terms of triggering regimes. Half of the M_w 7.0 earthquakes triggered mass flows. These cable breaks occurred just east of Amatique Bay, Guatemala. In the rest of the Caribbean there was no evidence of a mass flow triggered by an earthquake with a M_w > 5.5. The other flows triggered by low magnitude events occurred on river deltas along channels where turbidity currents have previously been identified. Cable breaks offshore Colombia occurred on the Magdalena Fan. Previous studies of the fan have shown that it regularly produces turbidity currents (Ercilla et al., 2002a, 2002b). Numerous historical cable breaks associated with this system have also been documented (Heezen, 1956). The cable break south of Jamaica also occurred in a region with an active turbidity current system (Burke, 1967). In these locations, it appears that earthquakes are one of multiple triggering mechanisms causing

mass flows but that high sediment supply is a vital component to their occurrence (Fig. 12b). In contrast, no earthquake triggered mass flows occur around the high seismicity regions of the Windward and Leeward Islands (Fig. 9). This is likely due to a lack of available sediment resulting from limited river catchments and transportation of sediment.

5.3.6. Pacific North America

The three strongest earthquakes in this region did not trigger mass flows (see Fig. 3). The strongest earthquake (M_w 7.5) which triggered a mass flow, resulted in the failure of the Stikine River delta (Wilt, 2015). This delta failure and the proglacial delta failure which was caused by a low M_w earthquake swarm clearly demonstrate the importance of sediment supply. Large numbers of cable breaks have also previously been identified in similar high sediment supply areas (see Fig. 12) in Western Canada and Alaska (Heezen and Johnson, 1969). However, the number of cables in this region has significantly decreased and thus the number of earthquake triggered flows which have not interacted with cables is likely much higher.

In terms of the regional picture of mass flow triggering a number of addition features must also be recognised. First, a number of earthquakes produced very different sedimentary responses offshore Mexico. Here, a M_w 6.0 earthquake triggered a cable breaking flow. However, neither a M_w 8.0 earthquake nor the M_w 7.6 in the same area triggered a mass flow. Assuming that the properties of the sediment did not drastically change, this observation is problematic for estimating which earthquakes should and should not trigger mass flows. Second, during the period of observation there was only 1 M_w 8.0 earthquake and none larger. Therefore the dataset of large magnitude events are too small to determine their capability to trigger mass flows.

5.4. Implications of the cable break database for turbidite palaeoseismology: linking deposits to earthquake magnitudes

Turbidite palaeoseismology relies on specific large earthquake magnitudes generating recognisable turbidites (Atwater and Griggs, 2012; Goldfinger et al., 2012; Gràcia et al., 2013; Atwater et al., 2014). For this to be robust, similar earthquakes of a given magnitude should generate similar deposits. The relationship between earthquake magnitudes and deposits does not have to be globally consistent. However, it does require regional consistency.

Our analysis of the cable break database shows there to be large regional variations in terms of the earthquake magnitudes which will trigger mass flows. These variations appear to be driven by a combination of the local seismicity and the supply of sediment. In order for turbidite palaeoseismology to be robust for a specific region, local sediment supply and slope response to earthquake shaking needs to be quantified.

It is also important to recognise that the cable break database has implied that local responses to earthquakes of the same magnitude are not always similar. Around Japan the cable break database suggests that only $\geq M_w$ 7.0 earthquakes will generate slope failures. Other studies using historical records around Japan support this conclusion as they find turbidites associated with known $\geq M_w$ 7.0 earthquakes (Noda et al., 2008; Shirai et al., 2010). However, the cable break database suggests that not all $\geq M_w$ 7.0 earthquakes produce mass flows. Therefore if it is assumed that all $\geq M_w$ 7.0 earthquakes produce mass flows and that such flows produce turbidites, then the palaeoseismology studies using cores will underestimate turbidite frequency and hence the frequency of $\geq M_w$ 7.0 earthquakes. These studies will also have to reconcile the problem of turbidites resulting from low magnitude earthquakes and earthquake swarms.

Quantifying uncertainties in turbidite palaeoseismology studies is extremely challenging. These uncertainties also directly affect our cable break analysis. Fig. 13 represents a possible Bayesian network for assessing the probability of an earthquake triggering a mass flow and it be detected by the cable network. We have not tried to assign probabilities to each node, nor define relationships between nodes.

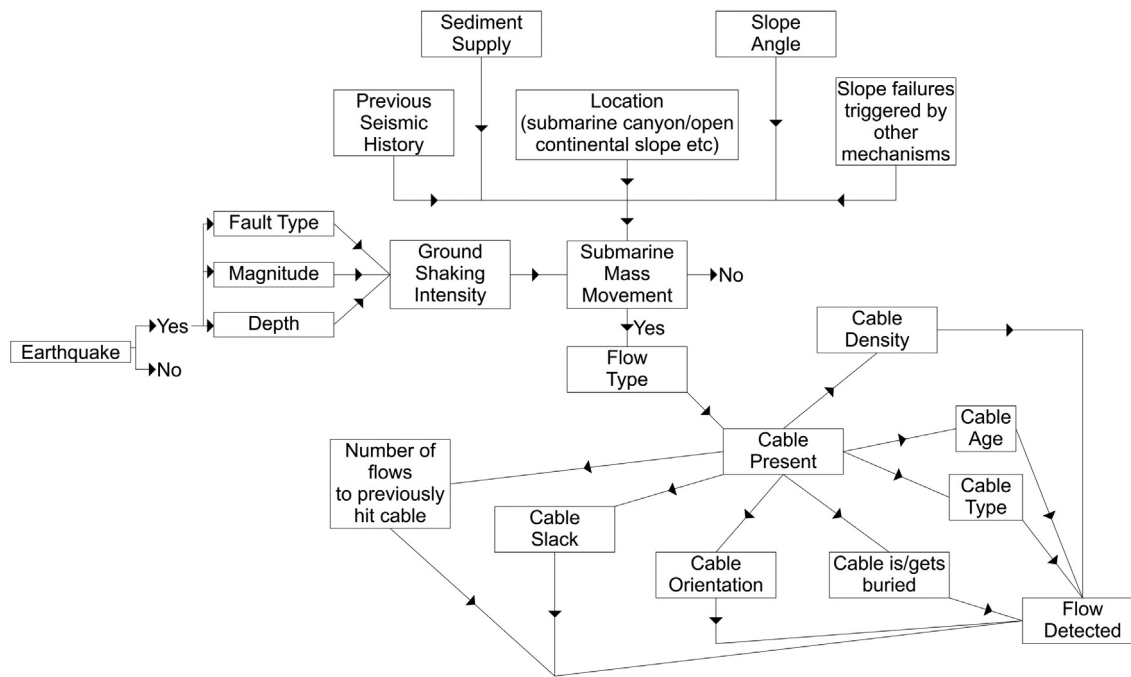


Fig. 13. A possible Bayesian network for assessing the probability that a cable would be broken by an earthquake triggered mass flow.

Currently we feel that any measurement of likelihood in a given scenario would be artificial. This is a result of the degree of uncertainty that still exists in terms of flow triggering and flow interaction with cable networks that we have outlined above. A more reliable application of Bayesian networks to the different areas could be made once local geological data regarding local geological conditions has been obtained. Once this is achieved, the results can be directly applied to future studies using cable breaks; information which can be subsequently applied to turbidite palaeoseismology studies.

6. Conclusions

Submarine mass movements are known to have several triggers. This study is the first to identify earthquake triggered submarine mass movements worldwide. The primary conclusion is that there is no obvious earthquake magnitude, which will consistently trigger a submarine mass flow. The only possible exception is that all M_w 9.0 earthquakes trigger submarine mass flows. However, the small number of M_w 9 earthquakes (2) is too small to make any robust conclusions.

Second, it appears that the relationship between earthquake magnitude, peak ground acceleration and the triggering of mass flow events varies on a regional basis. In some regions small magnitude (M_w 3.0 to 5.0) earthquakes can trigger mass flows whilst in others mass flows can only be triggered by large earthquakes ($\geq M_w$ 7.0). This is a response to variations in regional sediment supply, submarine topography, seismic regime and their temporal variability.

Third, not all earthquakes above a certain magnitude generate powerful (cable breaking) submarine mass movements. Indeed, globally only 15 of 56 (27%) earthquakes above M_w 7.0 produced mass flows that broke cables. This suggests that not all major earthquakes may produce powerful flows that cover large areas.

Subsea cables have been clearly shown to be an important means of detecting submarine mass flows. However, the use of cables has limitations that include (i) uneven distribution through the world ocean, (ii) only detect mass flows sufficiently powerful to break cables, (iii) several cables can respond differently to the same mass flow, i.e. some break whilst others remain intact, the causes of which are unclear and (iv) the absence of a fully comprehensive universal cable break database.

Acknowledgements

We are very grateful to Global Marine Systems Ltd. (GMSL) for access and permission to use its cable break database. In this regard, the assistance of Brian Perrat and Steve Holden of GMSL is particularly appreciated. General information on subsea telecommunications cables was generously supplied by the International Cable Protection Committee and its members. The project was supported by the NERC Environmental Risks to Infrastructure Innovation Programme (NE/N012798/1). P.J. Talling was supported by a NERC Royal Society Industry Fellowship to understand submarine sediment flows and the risk they pose to global telecommunications. This research was completed within the scope of the EU FP7-funded ASTARTE (Assessment, Strategy and Risk Reduction for Tsunamis in Europe) Project (603839). We thank the guest editor, Michael Strasser, and two reviewers, Hugo Pouderoux and Geoffroy Lamarche, whose helpful comments greatly improved the manuscript.

Appendix A. Supplementary data

Supplementary data to this article can be found online at <http://dx.doi.org/10.1016/j.margeo.2016.01.009>.

References

- Adams, J., 1990. Paleoseismicity of the Cascadia subduction zone: evidence from turbidites off the Oregon–Washington margin. *Tectonics* 9, 569–583.
- Allen, T.L., Wald, D.J., Earle, P.S., Marano, K.D., Hotovec, A.J., Lin, K., Hearne, M.G., 2009. An Atlas of ShakeMaps and population exposure catalog for earthquake loss modeling. *Bull. Earthq. Eng.* 7, 701–718.
- Ambraseys, N.N., Simpson, K.A., Bommer, J., 1996. Prediction of horizontal response spectra in Europe. *Earthq. Eng. Struct. Dyn.* 25, 371–400.
- Andrioux, O., Cooper, C.K., Wood, J., 2013. Turbidity Current Measurements in the Congo Canyon. Offshore Technology Conference. Offshore Technology Conference.
- Atwater, B.F., Griggs, G.B., 2012. Deep-sea turbidites as guides to Holocene earthquake history at the Cascadia Subduction Zone—alternative views for a seismic-hazard workshop. US Geological Survey Open-File Report 1043 p. 58.
- Atwater, B.F., Carson, B., Griggs, G.B., Johnson, H.P., Salmi, M.S., 2014. Rethinking turbidite paleoseismology along the Cascadia subduction zone. *Geology* 42, 827–830.
- Beck, C., De Lépinay, B.M., Schneider, J.-L., Cremer, M., Çağatay, N., Wendenbaum, E., Boutareaud, S., Ménot, G., Schmidt, S., Weber, O., 2007. Late Quaternary co-seismic sedimentation in the Sea of Marmara's deep basins. *Sediment. Geol.* 199, 65–89.

- Boe, R., Prosch-Danielsen, L., Lepland, A., Harbitz, C.B., Gauer, P., Lovholt, F., Hogestol, M., 2007. An early Holocene submarine slide in Boknafjorden and the effect of a slide-triggered tsunami on Stone Age settlements at Rennesøy, SW Norway. *Mar. Geol.* 243, 157–168.
- Boore, D.M., Atkinson, G.M., 2008. Ground-motion prediction equations for the average horizontal component of PGA, PGV, and 5%-damped PSA at spectral periods between 0.01 s and 10.0 s. *Earthquake Spectra* 24, 99–138.
- Burke, K., 1967. The Yallahs Basin: a sedimentary basin southeast of Kingston, Jamaica. *Mar. Geol.* 5, 45–60.
- Burnett, D.R., Beckman, R., Davenport, T.M., 2013. *Submarine Cables: The Handbook of Law and Policy*. Martinus Nijhoff Publishers.
- Camerlenghi, A., Urgeles, R., Fantoni, L., 2010. A database on submarine landslides of the Mediterranean Sea. *Submarine Mass Movements and Their Consequences*. Springer, pp. 503–513.
- Campbell, K.W., 1997. Empirical near-source attenuation relationships for horizontal and vertical components of peak ground acceleration, peak ground velocity, and pseudo-absolute acceleration response spectra. *Seismol. Res. Lett.* 68, 154–179.
- Campbell, K.W., 2003. Prediction of strong ground motion using the hybrid empirical method and its use in the development of ground-motion (attenuation) relations in eastern North America. *Bull. Seismol. Soc. Am.* 93, 1012–1033.
- Carter, L., Burnett, D., Drew, S., Hagadorn, L., Marle, G., Bertlett-McNeil, D., Irvine, N., 2009. Submarine cables and the oceans – connecting the world. UNEP-WCMC Biodiversity Series 31 G4. ICP/C/UNEP/UNEP-WCMC.
- Carter, L., Milliman, J.D., Talling, P.J., Gavey, R., Wynn, R.B., 2012. Near-synchronous and delayed initiation of long run-out submarine sediment flows from a record-breaking river flood, offshore Taiwan. *Geophys. Res. Lett.* 39.
- Cattaneo, A., Babonneau, N., Ratzov, G., Dan-Unterseh, G., Yelles, K., Bracene, R., De Lepinay, B.M., Boudiaf, A., Déverchère, J., 2012. Searching for the seafloor signature of the 21 May 2003 Boumerdes earthquake offshore central Algeria. *Nat. Hazards Earth Syst. Sci.* 12, 2159–2172.
- Chronis, G., Lykousis, V., Georgopoulos, D., Zervakis, V., Stavrakakis, S., Poulos, S., 2000. Suspended particulate matter and nepheloid layers over the southern margin of the Cretan Sea (NE Mediterranean): seasonal distribution and dynamics. *Prog. Oceanogr.* 46, 163–185.
- Cooper, C., Wood, J., Andrioux, O., 2013. Turbidity current measurements in the Congo Canyon. Offshore Technology Conference, pp. 06–09 (May).
- Dadson, S.J., Hovius, N., Chen, H., Dade, W.B., Lin, J.-C., Hsu, M.-L., Lin, C.-W., Horng, M.-J., Chen, T.-C., Milliman, J.D., 2004. Earthquake-triggered increase in sediment delivery from an active mountain belt. *Geology* 32, 733–736.
- Dan, G., Sultan, N., Savoye, B., Déverchère, J., Yelles, K., 2009. Quantifying the role of sandy-silty sediments in generating slope failures during earthquakes: example from the Algerian margin. *Int. J. Earth Sci.* 98, 769–789.
- Das, R., Wason, H.R., Sharma, M.L., 2011. Global regression relations for conversion of surface wave and body wave magnitudes to moment magnitude. *Nat. Hazards* 59, 801–810.
- Dengler, A.T., Wilde, P., Noda, E.K., Normark, W.R., 1984. Turbidity currents generated by Hurricane Iwa. *Geo-Mar. Lett.* 4, 5–11.
- Di Giacomo, D., Bondár, I., Storchak, D.A., Engdahl, E.R., Bormann, P., Harris, J.C., 2015. ISC-GEM: Global Instrumental Earthquake Catalogue (1900–2009), III. Re-computed M_s and m_b , proxy M_w , final magnitude composition and completeness assessment. *Phys. Earth Planet. Inter.* 239, 33–47.
- El-Robrini, M., Gennesseaux, M., Mauffret, A., 1985. Consequences of the El-Asnam earthquakes: turbidity currents and slumps on the Algerian margin (Western Mediterranean). *Geo-Mar. Lett.* 5, 171–176.
- Ercilla, G., Alonso, B., Estrada, F., Chiocci, F.L., Baraza, J., Li Farran, M., 2002a. The Magdalena Turbidite System (Caribbean Sea): present-day morphology and architecture model. *Mar. Geol.* 185, 303–318.
- Ercilla, G., Wynn, R.B., Alonso, B., Baraza, J., 2002b. Initiation and evolution of turbidity current sediment waves in the Magdalena turbidite system. *Mar. Geol.* 192, 153–169.
- Goldfinger, C., 2011. Submarine paleoseismology based on turbidite records. *Ann. Rev. Mar. Sci.* 3 (3), 35–66.
- Goldfinger, C., Nelson, C.H., Johnson, J.E., 2003. Holocene earthquake records from the Cascadia subduction zone and northern San Andreas fault based on precise dating of offshore turbidites. *Annu. Rev. Earth Planet. Sci.* 31, 555–577.
- Goldfinger, C., Nelson, C.H., Morey, A.E., Johnson, J.E., Patton, J.R., Karabarov, E., Gutierrez-Pastor, J., Eriksson, A.T., Gracia, E., Dunhill, G., 2012. Turbide Event History: Methods and Implications for Holocene Paleoseismicity of the Cascadia Subduction Zone. US Department of the Interior, US Geological Survey.
- Gracia, E., Lamarche, G., Nelson, H., Pantosti, D., 2013. Preface: marine and Lake paleoseismology. *Nat. Hazards Earth Syst. Sci.* 13, 3469–3478.
- Hafslidason, H., Lien, R., Sejrup, H.P., Forsberg, C.F., Bryn, P., 2005. The dating and morphometry of the Storegga Slide. *Mar. Pet. Geol.* 22, 123–136.
- Heezen, B.C., 1956. Corrientes de turbidez del Rio Magdalena. *Bol. Soc. Geol. Colombia* 51/52, 135–143.
- Heezen, B.C., Ewing, W.M., 1952. Turbidity currents and submarine slumps, and the 1929 Grand Banks [Newfoundland] earthquake. *Am. J. Sci.* 250, 849–873.
- Heezen, B.C., Ewing, M., 1955. Orleansville earthquake and turbidity currents. *AAPG Bull.* 39, 2505–2514.
- Heezen, B.C., Johnson, G.L., 1969. Alaskan submarine cables: a struggle with a harsh environment. *Arctic* 413–424.
- Heezen, B.C., Menzies, R.J., Schneider, E.D., Ewing, W.M., Granelli, N.C.L., 1964. Congo submarine canyon. *AAPG Bull.* 48, 1126–1149.
- Holzer, T.L., Savage, J.C., 2013. Global earthquake fatalities and population. *Earthquake Spectra* 29, 155–175.
- Hsu, S.K., Kuo, J., Lo, C.I., Tsai, C.H., Doo, W.B., Ku, C.Y., Sibuet, J.C., 2008. Turbidity currents, submarine landslides and the 2006 Pingtung Earthquake off SW Taiwan. *Terr. Atmos. Ocean. Sci.* 19, 767–772.
- Ide, S., Baltay, A., Beroza, G.C., 2011. Shallow dynamic overshoot and energetic deep rupture in the 2011 Mw 9.0 Tohoku-Oki earthquake. *Science* 332, 1426–1429.
- Kao, S.-J., Dai, M., Selvaraj, K., Zhai, W., Cai, P., Chen, S.-N., Yang, J., Liu, J., Liu, C., Syvitski, J.P., 2010. Cyclone-driven deep sea injection of freshwater and heat by hyperpycnal flow in the subtropics. *Geophys. Res. Lett.* 37.
- Keefe, D.K., 1984. Landslides caused by earthquakes. *Geol. Soc. Am. Bull.* 95, 406–421.
- Keefe, D.K., 2002. Investigating landslides caused by earthquakes—a historical review. *Surv. Geophys.* 23, 473–510.
- Khrapounoff, A., Vangriesheim, A., Babonneau, N., Crassous, P., Dennielou, B., Savoye, B., 2003. Direct observation of intense turbidity current activity in the Zaire submarine valley at 4000 m water depth. *Mar. Geol.* 194, 151–158.
- Krause, D.C., White, W.C., Piper, D.J.W., Heezen, B.C., 1970. Turbidity currents and cable breaks in the western New Britain Trench. *Geol. Soc. Am. Bull.* 81, 2153–2160.
- Lee, H.J., Schwab, W.C., Booth, J.S., 1993. Submarine landslides: an introduction. *Submarine Landslides: Selected Studies in the US Exclusive Economic Zone*, p. 1–1.
- Lee, H.J., Chough, S.K., Yoon, S.H., 1996. Slope-stability change from late Pleistocene to Holocene in the Ulleung Basin, East Sea (Japan Sea). *Sediment. Geol.* 104, 39–51.
- Lee, H.J., Locat, J., Dartnell, P., Israel, K., Wong, F., 1999. Regional variability of slope stability: application to the Elm margin, California. *Mar. Geol.* 154, 305–321.
- Liu, J.T., Kao, S.-J., Huh, C.-A., Hung, C.-C., 2013. Gravity flows associated with flood events and carbon burial: Taiwan as instructional source area. *Ann. Rev. Mar. Sci.* 5, 47–68.
- Lorenzon, L., Benitez-Nelson, C.R., Thunell, R.C., Hollander, D., Varela, R., Astor, Y., Audemard, F.A., Muller-Karger, F.E., 2012. Potential role of event-driven sediment transport on sediment accumulation in the Cariaco Basin, Venezuela. *Mar. Geol.* 307, 105–110.
- Lykousis, V., Roussakis, G., Alexandri, M., Pavlakis, P., Papoulia, I., 2002. Sliding and regional slope stability in active margins: North Aegean Trough (Mediterranean). *Mar. Geol.* 186, 281–298.
- Makdisi, F.I., Seed, H.B., 1977. Simplified procedure for estimating dam and embankment earthquake-induced deformations. ASAE Publication No. 4-77. Proceedings of the National Symposium on Soil Erosion and Sediment by Water, Chicago, Illinois, December 12–13, 1977.
- McAdoo, B.G., Watts, P., 2004. Tsunami hazard from submarine landslides on the Oregon continental slope. *Mar. Geol.* 203, 235–245.
- McAdoo, B.G., Pratson, L.F., Orange, D.L., 2000. Submarine landslide geomorphology, US continental slope. *Mar. Geol.* 169, 103–136.
- McHugh, C.M., Seeber, L., Braudy, N., Cormier, M.-H., Davis, M.B., Diebold, J.B., Dieudonne, N., Douilly, R., Gulick, S.P.S., Hornbach, M.J., 2011. Offshore sedimentary effects of the 12 January 2010 Haiti earthquake. *Geology* 39, 723–726.
- Meunier, P., Hovius, N., Haines, A.J., 2007. Regional patterns of earthquake-triggered landslides and their relation to ground motion. *Geophys. Res. Lett.* 34.
- Milliman, J.D., Farnsworth, K.L., 2011. River Discharge to the Coastal Ocean: A Global Synthesis. Cambridge University Press.
- Milliman, J.D., Meade, R.H., 1983. World-wide delivery of river sediment to the oceans. *J. Geol.* 1–21.
- Milliman, J.D., Syvitski, J.P.M., 1992. Geomorphic tectonic control of sediment discharge to the ocean – the importance of small mountainous rivers. *J. Geol.* 100, 525–544.
- Moernaut, J., Van Daele, M., Heirman, K., Fontijn, K., Strasser, M., Pino, M., Urrutia, R., De Batist, M., 2014. Lacustrine turbidites as a tool for quantitative earthquake reconstruction: new evidence for a variable rupture mode in south central Chile. *J. Geophys. Res. Solid Earth* 119, 1607–1633.
- Mulder, T., Syvitski, J.P.M., Migeon, S., Faugeres, J.-C., Savoye, B., 2003. Marine hyperpycnal flows: initiation, behavior and related deposits. A review. *Mar. Pet. Geol.* 20, 861–882.
- Nakajima, T., Kanai, Y., 2000. Sedimentary features of seismoturbidites triggered by the 1983 and older historical earthquakes in the eastern margin of the Japan Sea. *Sediment. Geol.* 135, 1–19.
- Nanayama, F., Furukawa, R., Shigeno, K., Makino, A., Soeda, Y., Igarashi, Y., 2007. Nine unusually large tsunami deposits from the past 4000 years at Kiritappu marsh along the southern Kuril Trench. *Sediment. Geol.* 200, 275–294.
- Nelson, A.R., Atwater, B.F., Bobrowsky, P.T., Bradley, L.-A., Clague, J.J., Carver, G.A., Darienzo, M.E., Grant, W.C., Krueger, H.W., Sparks, R.S.J., 1995. Radiocarbon evidence for extensive plate-boundary rupture about 300 years ago at the Cascadia subduction zone. *Nature* 378, 371–374.
- Niemi, T.M., Ben-Avraham, Z., 1994. Evidence for Jericho earthquakes from slumped sediments of the Jordan River delta in the Dead Sea. *Geology* 22, 395–398.
- Noda, A., TuZino, T., Kanai, Y., Furukawa, R., Uchida, J., 2008. Paleoseismicity along the southern Kuril Trench deduced from submarine-fan turbidites. *Mar. Geol.* 254, 73–90.
- Owen, L.A., Kamp, U., Khattak, G.A., Harp, E.L., Keefer, D.K., Bauer, M.A., 2008. Landslides triggered by the 8 October 2005 Kashmir earthquake. *Geomorphology* 94, 1–9.
- Parker, E.J., Traverso, C.M., Giudice, T.D., Evans, T., Moore, R., 2009. Geohazard risk assessment – vulnerability of subsea structures to geohazards – risk implications. Proceedings of the Offshore Technology Conference, 2009, Houston, Texas.
- Patton, J.R., Goldfinger, C., Morey, A.E., Romsos, C., Black, B., Djadjadihardja, Y., 2013. Seismoturbidite record as preserved at core sites at the Cascadia and Sumatra-Andaman subduction zones. *Nat. Hazards Earth Syst. Sci.* 13, 833–867.
- Piper, D.J.W., Normark, W.R., 2009. Processes that initiate turbidity currents and their influence on turbidites: a marine geology perspective. *J. Sediment. Res.* 79, 347–362.
- Piper, D.J.W., Cochonat, P., Morrison, M.L., 1999. The sequence of events around the epicentre of the 1929 Grand Banks earthquake: initiation of debris flows and turbidity current inferred from sidescan sonar. *Sedimentology* 46, 79–97.
- Pouderoux, H., Lamarche, G., Proust, J.-N., 2012. Building an 18 000-year-long paleo-earthquake record from detailed deep-sea turbidite characterisation in Poverty Bay, New Zealand. *Nat. Hazards Earth Syst. Sci.* 12, 2077–2101.

- Pouderoux, H., Proust, J.-N., Lamarche, G., 2014. Submarine paleoseismology of the northern Hikurangi subduction margin of New Zealand as deduced from turbidite record since 16 ka. *Quat. Sci. Rev.* 84, 116–131.
- Ramsey, L.A., Hovius, N., Lague, D., Liu, C.S., 2006. Topographic characteristics of the submarine Taiwan orogen. *J. Geophys. Res. Earth Surf.* 2003–2012, 111.
- Ratzov, G., Cattaneo, A., Babonneau, N., Déverchère, J., Yelles, K., Bracene, R., Courboulex, F., 2015. Holocene turbidites record earthquake supercycles at a slow-rate plate boundary. *Geology* 43, 331–334.
- Scardiis, E.M., 2006. Empirical global relations converting M_S and m_b to moment magnitude. *J. Seismol.* 10, 225–236.
- Seed, H.B., Idriss, I.M., 1971. Simplified procedure for evaluating soil liquefaction potential. *J. Soil Mech. Found. Div.* 97, 1249–1273.
- Shanmugam, G., 2008. Deep-water bottom currents and their deposits. *Dev. Sedimentol.* 60, 59–81.
- Shirai, M., Omura, A., Wakabayashi, T., Uchida, J., Ogami, T., 2010. Depositional age and triggering event of turbidites in the western Kumano Trough, central Japan during the last ca. 100 years. *Mar. Geol.* 271, 225–235.
- Si, H., Midorikawa, S., 1999. New attenuation relationships for peak ground acceleration and velocity considering effects of fault type and site condition. *J. Struct. Constr. Eng.* 63–70.
- Stigall, J., Dugan, B., 2010. Overpressure and earthquake initiated slope failure in the Ursula region, northern Gulf of Mexico. *J. Geophys. Res. Solid Earth* 115.
- Strasser, M., Anselmetti, F.S., Fäh, D., Giardini, D., Schnellmann, M., 2006. Magnitudes and source areas of large prehistoric northern Alpine earthquakes revealed by slope failures in lakes. *Geology* 34, 1005–1008.
- Strasser, M., Kölling, M., dos Santos Ferreira, C., Fink, H.G., Fujiwara, T., Henkel, S., Ikehara, K., Kanamatsu, T., Kawamura, K., Kodaira, S., 2013. A slump in the trench: tracking the impact of the 2011 Tohoku-Oki earthquake. *Geology* 41, 935–938.
- Strozyk, F., Strasser, M., Förster, A., Kopf, A., Huhn, K., 2010. Slope failure repetition in active margin environments: constraints from submarine landslides in the Hellenic fore arc, eastern Mediterranean. *J. Geophys. Res. Solid Earth* 1978–2012, 115.
- Su, C.-C., Tseng, J.-Y., Hsu, H.-H., Chiang, C.-S., Yu, H.-S., Lin, S., Liu, J.T., 2012. Records of submarine natural hazards off SW Taiwan. *Geol. Soc. Lond. Spec. Publ.* 361, 41–60.
- Sultan, N., Cochonat, P., Canals, M., Cattaneo, A., Dennielou, B., Hafstadson, H., Laberg, J.S., Long, D., Mienert, J., Trincardi, F., Urgeles, R., Vorren, T.O., Wilson, C., 2004. Triggering mechanisms of slope instability processes and sediment failures on continental margins: a geotechnical approach. *Mar. Geol.* 213, 291–321.
- Sumner, E.J., Siti, M.I., McNeill, L.C., Talling, P.J., Henstock, T.J., Wynn, R.B., Djajadihardja, Y.S., Permana, H., 2013. Can turbidites be used to reconstruct a paleoearthquake record for the central Sumatran margin? *Geology* 41, 763–766.
- Talling, P.J., 2014. On the triggers, resulting flow types and frequencies of subaqueous sediment density flows in different settings. *Mar. Geol.* 352, 155–182.
- Talling, P.J., Masson, D.G., Sumner, E.J., Malgesini, G., 2012. Subaqueous sediment density flows: depositional processes and deposit types. *Sedimentology* 59, 1937–2003.
- Talling, P.J., Clare, M.A., Urlaub, M., Pope, E., Hunt, J.E., Watt, S.F.L., 2014. Large submarine landslides on continental slopes. *Oceanography* 27, 32.
- Tappin, D.R., Watts, P., McMurtry, G.M., Lafay, Y., Matsumoto, T., 2001. The Sissano, Papua New Guinea tsunami of July 1998 – offshore evidence on the source mechanism. *Mar. Geol.* 175, 1–23.
- Tappin, D.R., Grilli, S.T., Harris, J.C., Geller, R.J., Masterlark, T., Kirby, J.T., Shi, F., Ma, G., Thingbaijam, K.K.S., Mai, P.M., 2014. Did a submarine landslide contribute to the 2011 Tohoku tsunami? *Mar. Geol.* 357, 344–361.
- ten Brink, U.S., Chaytor, J.D., Geist, E.L., Brothers, D.S., Andrews, B.D., 2014. Assessment of tsunami hazard to the US Atlantic margin. *Mar. Geol.* 353, 31–54.
- Tinti, S., Armigliato, A., Manucci, A., Pagnoni, G., Zaniboni, F., Yalçiner, A.C., Altinok, Y., 2006. The generating mechanisms of the August 17, 1999 Izmit Bay (Turkey) tsunami: regional (tectonic) and local (mass instabilities) causes. *Mar. Geol.* 225, 311–330.
- Vanoudheusden, E., Sultan, N., Cochonat, P., 2004. Mechanical behaviour of unsaturated marine sediments: experimental and theoretical approaches. *Mar. Geol.* 213, 323–342.
- Völker, D., Scholz, F., Geersen, J., 2011. Analysis of submarine landsliding in the rupture area of the 27 February 2010 Maule earthquake, Central Chile. *Mar. Geol.* 288, 79–89.
- Wald, D.J., Quitoriano, V., Heaton, T.H., Kanamori, H., Scrivner, C.W., Worden, C.B., 1999. TriNet "ShakeMaps": rapid generation of peak ground motion and intensity maps for earthquakes in southern California. *Earthquake Spectra* 15, 537–555.
- Wald, D.J., Worden, B.C., Quitoriano, V., Pankow, K.L., 2005. ShakeMap Manual: Technical Manual, User's Guide, and Software Guide. US Geological Survey, Reston, VA, p. 132.
- Wald, D.J., Lin, K.-W., Quitoriano, V., 2008. Quantifying and qualifying USGS ShakeMap uncertainty. US Geological Survey Open-File Report 2008 – 1238. Geological Survey (US), Golden, CO, p. 27.
- Wells, D.L., Coppersmith, K.J., 1994. New empirical relationships among magnitude, rupture length, rupture width, rupture area, and surface displacement. *Bull. Seismol. Soc. Am.* 84, 974–1002.
- Wilt, G.G., 2015. A study of delta collapse caused turbidity current cable failures. International Cable Protection Committee Plenary, Enhanced Submarine Cable Security and Co-operation in Balance with the Environment, Hong Kong, China.
- Xu, J.P., Sequeiros, O.E., Noble, M.A., 2014. Sediment concentrations, flow conditions, and downstream evolution of two turbidity currents, Monterey Canyon, USA. *Deep-Sea Res. I Oceanogr. Res. Pap.* 89, 11–34.